EJN fens European Journal of Neuroscience

European Journal of Neuroscience, Vol. 31, pp. 286–301, 2010 doi:10.1111/j.1460-9568.2009.07054.x

NEUROSYSTEMS

Cannabinoid modulation of limbic forebrain noradrenergic circuitry

Ana F. Carvalho,[1,2] Kenneth Mackie[3] and Elisabeth J. Van Bockstaele[1]
[1]Neurosurgery, Farber Institute for Neurosciences, Thomas Jefferson University, 900 Walnut Street, Suite 417, Philadelphia, PA 19107, USA
[2]Life and Health Sciences Research Institute (ICVS), School of Health Sciences, University of Minho, Braga, Portugal
[3]Psychological and Brain Sciences, Indiana University, Bloomington, IN, USA

Keywords: adrenergic receptor, cannabinoid receptor type 1, nucleus accumbens, nucleus of the solitary tract, Sprague–Dawley

Abstract

Both the endocannabinoid and noradrenergic systems have been implicated in neuropsychiatric disorders. Importantly, low levels of norepinephrine are seen in patients with depression, and antagonism of the cannabinoid receptor type 1 (CB1R) is able to induce depressive symptoms in rodents and humans. Whether the interaction between the two systems is important for the regulation of these behaviors is not known. In the present study, adult male Sprague–Dawley rats were acutely or chronically administered the CB1R synthetic agonist WIN 55,212-2, and α2A and β1 adrenergic receptors (AR) were quantified by Western blot. These AR have been shown to be altered in a number of psychiatric disorders and following antidepressant treatment. CB1R agonist treatment induced a differential decrease in α2A- and β1-ARs in the nucleus accumbens (Acb). Moreover, to assess long-lasting changes induced by CB1R activation, some of the chronically treated rats were killed 7 days following the last injection. This revealed a persistent effect on α2A-AR levels. Furthermore, the localization of CB1R with respect to noradrenergic profiles was assessed in the Acb and in the nucleus of the solitary tract (NTS). Our results show a significant topographic distribution of CB1R and dopamine beta hydroxylase immunoreactivities (ir) in the Acb, with higher co-localization observed in the NTS. In the Acb, CB1R-ir was found in terminals forming either symmetric or asymmetric synapses. These results suggest that cannabinoids may modulate noradrenergic signaling in the Acb, directly by acting on noradrenergic neurons in the NTS or indirectly by modulating inhibitory and excitatory input in the Acb.

Introduction

The cannabinoid receptor type 1 (CB1R) can be found in several areas of the brain such as the frontal cortex, basal ganglia, hippocampus, amygdala and brainstem (Mackie, 2005), and it has been implicated in the regulation of learning and memory as well as in depression, anxiety and pain. CB1R activation is known to inhibit GABA and glutamate release in several brain regions, including the hippocampus, dorsal striatum, cerebellum and nucleus accumbens (Acb; Hoffman & Lupica, 2000; Daniel & Crepel, 2001; Gerdeman & Lovinger, 2001; Robbe *et al.*, 2001). In addition to the effects of cannabinoids on GABA and glutamate transmission, growing evidence points to a significant role for monoamines in cannabinoid-induced behaviors. Previous studies have shown important interactions between the cannabinoid and noradrenergic systems (Oropeza *et al.*, 2005, 2007; Page *et al.*, 2007; Fox *et al.*, 2009; Jelsing *et al.*, 2009). Systemic administration of the synthetic cannabinoid agonist WIN 55,212-2 was shown to increase the release of norepinephrine (NE) in the prefrontal cortex (PFC) (Oropeza *et al.*, 2005). In addition, WIN 55,212-2 increased c-fos expression in the locus coeruleus (LC) and in the nucleus of the solitary tract (NTS; Oropeza *et al.*, 2005; Jelsing *et al.*, 2009). Efferents of the LC and the NTS account for most of the noradrenergic projections to the forebrain. The noradrenergic input to cortical and limbic structures is important for brain arousal, memory and mood (Aston-Jones *et al.*, 1991; Heninger *et al.*, 1996). Dysregulation of this system plays a role in the pathophysiology of depression (Heninger *et al.*, 1996; Anand & Charney, 2000; Nutt, 2002). Noradrenergic deficiency and dysfunction of adrenergic receptors (AR) may be present in some patients with depression and may be important for the response to antidepressants (Anand & Charney, 2000). Consistent with this, various studies show an increase in α2-AR density in brains of depressed suicide victims (Meana *et al.*, 1992; De Paermentier *et al.*, 1997; Callado *et al.*, 1998) while β1-AR density is decreased (De Paermentier *et al.*, 1990). With regard to antidepressant treatment, the levels of α2- and β1-ARs have been shown to decrease (De Paermentier *et al.*, 1991, 1997) in areas such as temporal cortex, amygdala and thalamus of antidepressant-treated suicides. Moreover, chronic administration of WIN 55,212-2 has been shown to desensitize α2-ARs in noradrenergic-enriched areas (Moranta *et al.*, 2009). Elucidating the effects of cannabinoid administration on the expression of these ARs may contribute to

Correspondence: A. F. Carvalho, [1]Neurosurgery, as above.
E-mail: arfranky@gmail.com

Received 21 July 2009, revised 30 October 2009, accepted 10 November 2009

identifying the mechanism by which cannabinoids are involved in mood-related disorders (Hill & Gorzalka, 2005a; Witkin *et al.*, 2005; Leweke & Koethe, 2008).

In the present study, we studied the impact of a cannabinoid agonist on limbic forebrain noradrenergic circuitry using biochemical and neuroanatomical approaches. The limbic region analyzed, the Acb, is a brain region involved in the integration of motivation-related information, with important implications for drug addiction and mood disorders (Di Chiara, 2002; Shirayama & Chaki, 2006). Understanding how cannabinoids may impact noradrenergic input to the Acb may provide important information regarding the effects of CB1R compounds on drug-induced behaviors.

Materials and methods

Subjects

Adult male Sprague–Dawley rats (Harlan Laboratories, Indianapolis, IN, USA) weighing 220–250 g were housed two or three per cage in a controlled environment (12-h light schedule, temperature at 20°C). Food and water were provided *ad libitum*. The care and use of animals were approved by the Institutional Animal Care and Use Committee (IACUC) of Thomas Jefferson University and were conducted in accordance with the NIH *Guide for the care and use of laboratory animals.* All efforts were made to reduce the number of animals used.

Antibody characterization and specificity

A list with the characterization of all the primary antibodies used can be found in Table 1. An affinity-purified polyclonal antibody directed against the CB1R was used; it was generated against a fusion protein containing the last 15 amino acids of the C-terminal of the rat CB1R fused to glutathione *S*-transferase. The specificity of this CB1R antibody has been determined in somatosensory cortex of mice lacking CB1R by Bodor *et al.* (2005). In addition to the aforementioned study, additional controls were conducted here. For example, immunoperoxidase detection of the CB1R antibody was conducted in tissue sections obtained from the forebrain of mice deficient in the CB1R (provided by Kenneth Mackie) and compared to that of similar sections obtained from wild-type mice. In these experiments, peroxidase detection for CB1R was absent in knockout tissue but present in wild-type samples (Fig. 1). In addition, specificity controls involved controlling for the secondary antibody by processing tissue that lacked primary antibody incubation. In such experiments, run in parallel, peroxidase immunoreactivity or immunogold–silver particles were not detected in tissue sections from which the primary antibody had been omitted (Supporting information, Fig. S1). To evaluate possible cross-reactivity of secondary antibodies with the primary antisera in the dual labeling experiments, some sections were processed for dual labeling with omission of one of the primary antisera.

The monoclonal antibody against dopamine beta hydroxylase (DBH) was raised against purified bovine DBH. The specificity of the DBH antibody has also been demonstrated previously in our laboratory (Oropeza *et al.*, 2007). More specifically, preabsorption with the respective antigen (Alpha Diagnostics, San Antonio, TX, USA) resulted in an absence of immunolabeling in tissue sections from the frontal cortex.

The monoclonal (clone CL-300) antibody directed against calbindin was generated using purified calbindin-D from chicken gut. This antibody revealed the same distribution in the Acb as described by others (Voorn *et al.*, 1989; Jongen-Relo *et al.*, 1994).

The monoclonal antibody direct against the NE transporter (NET) was generated using a peptide (amino acids 05–17) of the mouse and rat NET coupled to keyhole limpet hemocyanin by the addition of a C-terminal cysteine. To test the specificity of the NET antibody, preabsorption of the antibody with the blocking peptide (1 μg/mL; MabTechnologies, Stone Mountain, GA, USA) resulted in the absence of immunolabeling in rat tissues containing the Acb (supporting Fig. S2).

The polyclonal antibody against the α2A-AR was developed against a synthetic peptide (Arg-Ile-Tyr-Gln-Ile-Ala-Lys-Arg-Arg-Thr-Arg-Val-Pro-Pro-Ser-Arg-Arg-Gly) derived from amino acids 218–235 of human, mouse, rat and pig α2A-AR. The polyclonal antibody against the β1-AR was raised against a synthetic peptide (His-Gly-Asp-Arg-Pro-Arg-Ala-Ser-Gly-Cys-Leu-Ala-Arg-Ala-Gly) derived from amino acids 394–408 of mouse and rat β1-AR. The specificity of α2A- and β1-AR antibodies was determined by preabsorption of the antibodies with the respective blocking peptide (10 μg/mL; Sigma-Aldrich, St Louis, MO, USA); this resulted in the absence of labeling in the blots loaded with whole-brain protein samples (supporting Fig. S3).

The monoclonal antibody against microtubule-associated protein (MAP2) was raised in mouse against rat brain MAP. The specificity of the MAP2 antibody has been described (Teng *et al.*, 2001), who found no detectable band in Western blots from brain extracts of MAP2-deficient mice.

Drug administration and Western blot analysis

WIN 55,212-2 (Sigma-Aldrich) was dissolved in 5% dimethyl sulfoxide (DMSO; Fisher Scientific, Fair Lawn, NJ, USA) in 0.9% saline and injected intraperitoneally in a volume of 1 mL/kg body weight. A dose–response study was performed in which animals

Table 1. Characterization of the primary antibodies

Antigen	Immunogen	Manufacturer	Host, mono/polyclonal	Catalog no.	Dilution
CB1R	Last 15 aa of the C-terminal of the rat CB1R	Dr K. Mackie*	Rabbit polyclonal	–	1:500 1:1000
DBH	Purified bovine DBH	Chemicon, Millipore	Mouse monoclonal	MAB308	1:1000
Calbindin D-28	Purified calbindin D-28 from chicken gut	Abcam	Mouse monoclonal	ab9481	1:300
NET	Peptide, aa 5–17 of mouse and rat NET	MabTechnologies	Mouse monoclonal	NET05-1	1:1000
α2A-AR	Synthetic peptide, aa 218–235 of human, mouse, rat and pig	Sigma-Aldrich	Rabbit polyclonal	A-271	1:500
β1-AR	Synthetic peptide, aa 394–408 of mouse and rat	Sigma-Aldrich	Rabbit polyclonal	A-272	1:1000
MAP2	Rat brain MAP	Abcam	Mouse monoclonal	ab11267	1:1000

*Synthesized in the laboratory of Dr K. Mackie; Chemicon, Millipore, Bedford, MA, USA; Abcam, Cambridge, MA, USA; MabTechnologies, Stone Mountain, GA, USA; Sigma-Aldrich, St Louis, MO, USA.

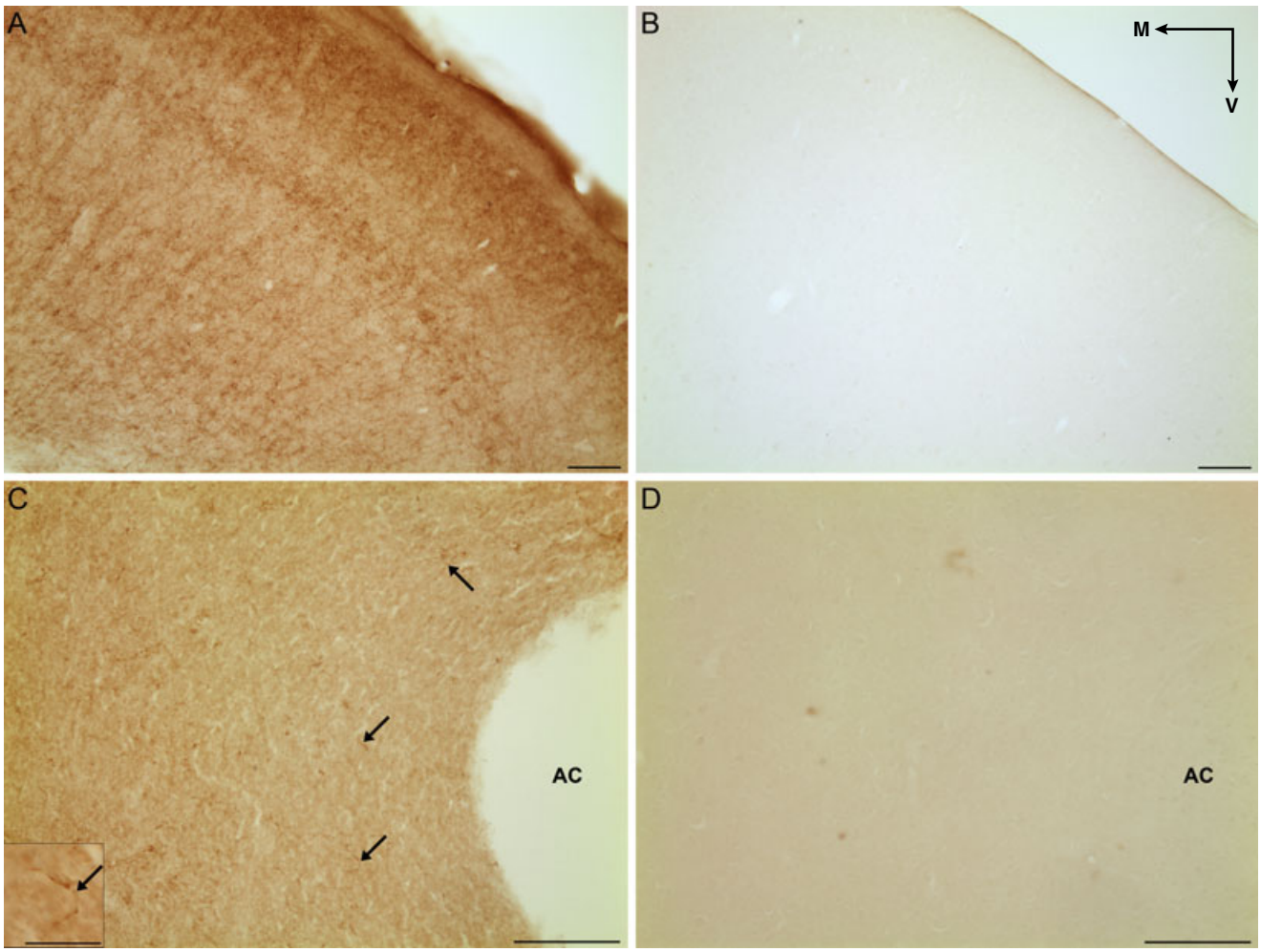

FIG. 1. Specificity of CB1R primary antibody. (A and C) Brightfield photomicrographs showing immunoperoxidase labeling for CB1R in a cross-section of (A) the frontal cortex (FC) and (C) the Acb (arrows) of a wild-type mouse brain. (B and D) Immunohistochemistry for CB1R in equivalent cross-sections of a CB1R-knockout mouse reveals an absence of immunolabeling in (B) the FC and (D) the Acb. Inset in C shows higher magnification of CB1R-labelled fiber indicated in C. AC, anterior commissure; M, medial; V, ventral. Scale bar, 100 μm.

received an acute injection of WIN 55,212-2 at 0.3, 1.0, 3.0 or 7.0 mg/kg (n = 20) or vehicle (5% DMSO in saline, n = 5). Another set of animals was divided into three treatment groups (acute, chronic and chronic + abstinence). In the acute group, animals received one injection of 3.0 mg/kg WIN 55,212-2 (n = 8) or vehicle (n = 6). The chronic group received a daily injection of WIN 55,212-2 (n = 8) or vehicle (n = 6) for 7 days. Animals in the dose–response study and in the acute and chronic groups were killed 40–45 min after the last injection. The chronic + abstinence group received repeated injections (7 days) of WIN 55,212-2 (n = 8) or vehicle (n = 6) and were killed 7 days after the last injection. Experimental animals were anesthetized with isoflurane (Isoflurane, USP; Webster Veterinary, Sterling, MA, USA) and decapitated. Brains were removed and a coronal section containing the whole extension of the Acb (from ~0.7 to 2.7 mm anterior to bregma) was cut. The area punched was located medially to the anterior commissure and ventrally to the lateral ventricle, and included the shell and medial core of the Acb (as shown in Fig. 2). Part of the cerebellum was also collected from a coronal section from ~10.50 to 12 mm posterior to bregma. Proteins were extracted in radio immunoprecipitation assay lysis buffer (Santa Cruz Biotechnology, Santa Cruz, CA, USA). Protein quantification was performed using the bicinchoninic acid reagent. Protein samples were loaded at equal concentrations and run on a 4–12% Tris-glycine gel (Invitrogen, Carlsbad, CA, USA). Gels were then transferred to Immobilon-P polyvinylidene difluoride membranes (Millipore Corp., Bedford, MA, USA) at 25 V for 2 h. Membranes were probed for rabbit anti-α2A-AR (1 : 500; Sigma-Aldrich), rabbit anti-β1-AR (1 : 1000; Sigma-Aldrich) or mouse anti-NET (1 : 5000; MabTechnologies) using the Western Breeze Chemilluminescent Kit (Invitrogen). In order to control for protein loading, each blot was stripped using Restore Stripping Buffer (Pierce, Rockford, IL, USA) and re-probed for β-actin (1 : 5000; Sigma-Aldrich).

Light microscopy and immunofluorescence

Seven naïve animals were used for light and immunofluorescence microscopy. Animals were deeply anesthetized with sodium pentobarbital (60 mg/kg), administered intraperitoneally, and transcardially perfused with 50 mL of heparinized saline followed by 400 mL of 4% formaldehyde (Electron Microscopy Sciences, Fort Washington, PA, USA) in 0.1 M phosphate buffer (PB; pH 7.4). After perfusion, brains were removed and postfixed in the same fixative. Coronal sections throughout the Acb and the NTS were cut at 40 μm using a Vibratome

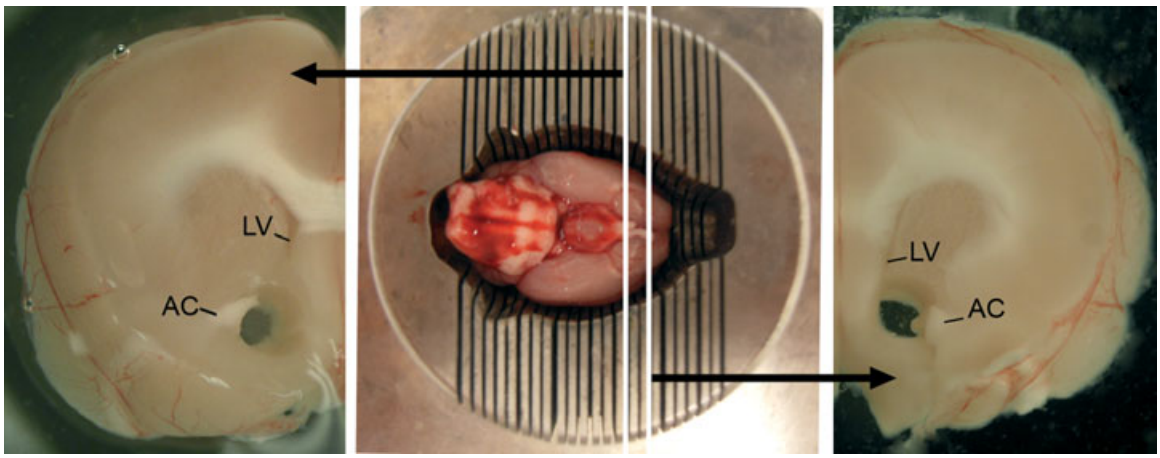

FIG. 2. Representative photomicrographs of the region of the Acb excised for protein analysis. A coronal section, ranging from just rostral to the optic chiasm to 2 mm anterior, was obtained in order to include the entire rostrocaudal extent of the Acb. Bilateral punches of the Acb were performed using a trephine medially to the anterior commissure (AC) and ventrally to the lateral ventricle (LV).

(Technical Product International, St Louis, MO, USA) and collected into 0.1 M PB. Every sixth section of the Acb was processed for immunohistochemical visualization of calbindin, CB1R or DBH immunoreactivities. Free-floating sections were treated with 1% sodium borohydride in 0.1 M PB for 30 min. They were then rinsed with 0.1 M PB and later washed in 0.1 M Tris saline buffer (TS; pH 7.6). The sections were blocked in 0.5% bovine serum albumin (BSA) in 0.1 M TS for 30 min and then washed for 5 min, twice. Sections were incubated overnight at room temperature with a mouse antibody for calbindin (1:300; Abcam, Cambridge, MA, USA), a rabbit antibody directed against CB1R (1:500) or a mouse monoclonal antibody recognizing DBH (1:1000; Chemicon, Millipore) in 0.1% BSA with 0.25% Triton-X 100 in 0.1 M TS. The sections were then washed in 0.1 M TS, three times for 10 min. Then, sections were incubated in a secondary biotin-conjugated donkey antirabbit or donkey antimouse IgG (1 : 400; Jackson ImmunoResearch, West Grove, PA, USA) in 0.1% BSA with 0.25% Triton-X 100 in 0.1 M TS for 30 min at room temperature. Then sections were washed in 0.1 M TS, three times for 10 min. Sections were incubated in an avidin–biotin complex solution (VECTASTAIN Elite ABC Kit; Vector Laboratories, Burlingame, CA, USA) in 0.1 M TS for 30 min and then washed. CB1R and DBH immunoreactivity was visualized with a red reaction by incubating the tissue sections in a red peroxidase substrate (VECTOR NovaRED substrate kit; Vector Laboratories) for 5 min, while the calbindin immunoreactivity was visualized with a blue reaction by incubating the sections in a blue peroxidase substrate (VECTOR SG substrate kit) for 10 min. The reaction was stopped by rinsing the sections in distilled water and then the sections were washed in 0.1 M TS. For dual immunofluorescence, every sixth section of Acb and NTS was processed as described above except that tissues were incubated overnight in a cocktail with rabbit anti-CB1R (1 : 500 for Acb sections, 1 : 5000 for NTS sections) and mouse anti-DBH antibodies or rabbit anti-CB1R and mouse anti-MAP2 (1 : 1000; Abcam) in 0.1% BSA+2% TritonX- 100 in 0.1 M TS. Tissue sections were then incubated in a secondary antibody solution containing fluorescein isothiocyanate donkey antimouse IgG (1 : 200; Jackson ImmunoResearch) and tetramethyl rhodamine isothiocyanate antirabbit IgG (1 : 400; Jacskon ImmunoResearch) in 0.1% BSA+2% Triton-X 100 in 0.1 M TS, for 2 h at room temperature. Sections were then washed in 0.1 M PB. Both dual- and single-labeled sections were mounted onto gelatinized glass slides from a 0.05 M PB solution. The slides were dehydrated through a graded series of alcohols and cleared in xylene before being coverslipped with Permount (light microscopy; Fisher Scientific, Pittsburgh, PA, USA) or DPX (immunofluorescence; Sigma-Aldrich) mounting mediums.

Electron microscopy

Although DBH was an adequate marker for noradrenergic terminals using light and fluorescence microscopy because it was possible to increase penetration with detergents in thicker tissue sections, this vesicular-bound enzyme was more difficult to consistently detect using electron microscopy with low concentrations of permeabilization agents. Therefore, without using detergents, NET was used as a marker to detect noradrenergic axon terminals and did not compromise the ultrastructural preservation of the neuropil. NET and CB1R were visualized in sections through the Acb obtained from naïve rats (n = 7) that were perfused with 50 mL of heparinized saline followed by 100 mL 3.8% acrolein (Electron Microscopy Sciences) and 400 mL of 2% formaldehyde (Electron Microscopy Sciences) in 0.1 M PB. Sections were processed following the protocol described for light microscopy except that Triton-X 100 was not added to the solution for antibody incubation. The sections were incubated overnight, at room temperature, in a primary antibody solution containing rabbit anti-CB1R (1 : 500) and mouse anti-NET (1 : 1000) with 0.1%BSA in 0.1 M TS. The NET antibody was visualized using immunoperoxidase detection by incubating sections in biotinylated donkey antimouse IgG (1 : 400; Jackson ImmunoResearch Laboratories) followed by avidin–biotin complex (Vector Laboratories). The sections were then reacted with 22 mg of 3-3′ diaminobenzidine (DAB; Sigma-Aldrich) containing 0.05% hydrogen peroxide for 15 min. For immunogold detection of CB1R, sections were then incubated in ultrasmall gold-conjugated goat antirabbit IgG (1 : 50; Electron Microscopy Sciences) with 0.8% BSA in 0.01 M PBS containing 0.1% fish gelatin (Amerhsam Corp., Amerhsam, UK) for 2 h. Sections were rinsed in the same buffer and then rinsed in 0.01 M PBS and incubated in 2% glutaraldehyde (Electron Microscopy Sciences) in 0.01 M PBS for 10 min, followed by washes in 0.01 M PBS and 0.2 M sodium citrate buffer (pH 7.4). A silver enhancement kit (Amersham Corp.) was used for silver intensification of the gold particles. Following intensification, tissue was rinsed in 0.1 M PB and incubated in 2% osmium tetroxide in 0.1 M PB for 1 h, washed in 0.1 M PB, dehydrated and flat-embedded in Epon 812 (Electron Microscopy Sciences). The reverse labeling was performed in which

CB1R was visualized by immunoperoxidase detection by using biotinylated donkey antirabbit (1 : 400; Jackson ImmunoResearch Laboratories) and immunogold detection of NET was visualized by ultrasmall gold-conjugated goat antimouse IgG (1 : 50; Electron Microscopy Sciences). Thin sections of 74 nm in thickness from the mid-ventral shell of the Acb were cut using diamond knife and collected on copper mesh grids.

Controls

For Western blot analysis, in order to minimize differences in the areas excised for protein extraction, the same investigator conducted the tissue dissection. To minimize protein loading errors, all gels run were loaded by the same person.

For immunohistochemical experiments, to control for specificity of the secondary antibodies, controls in which the primary antisera was omitted were run in parallel. Sections processed in the absence of primary antibody did not exhibit immunoreactivity. To evaluate cross-reactivity of labeling of the primary antiserum by secondary antisera, some sections were processed for dual labeling with omission of one of the primary antisera. To assure that DBH and NET stained the same profiles, dual immunofluorescence for DBH and NET was performed in tissue sections containing the Acb as described before (supporting Fig. S4).

Data analysis

Western blot

Blots were scanned into a PC computer and band intensities were quantified using Kodak Molecular Imaging Software (Version 4.5; Carestream Health Inc., Rochester, NY, USA). Intensities of bands for the adrenergic receptor proteins were normalized to that of β-actin in the same sample. Average intensity of bands for acute control tissues was arbitrarily set at 1. Statistical analysis was performed using SPSS 16.0 Graduate Student Version. Statistical analysis of data from the dose–response study was conducted using a one-way ANOVA followed by *post hoc* Bonferroni (with significance set at $P < 0.05$). For the analysis of the effects of acute, chronic and abstinence, a 2×3 ANOVA on the interaction between drug treatment (vehicle and drug) and treatment duration (acute, chronic and abstinence) was conducted. When a significant interaction was observed between the two factors, simple effects tests were conducted and a Bonferronni correction was applied. The results are expressed normalized to vehicle group values and SEM values are given.

Light microscopy

Slides with single-labeled sections were visualized using a Leica DMRBE microscope (Wetzlar, Germany), and images were acquired using SPOT Advanced software (Diagnostics Instruments, Inc., Sterling Heights, MI, USA). Figures were then assembled and adjusted for brightness and contrast in Adobe Photoshop CS2. Schematics showing the distribution of CB1R and DBH immunoreactivity are represented on coronal diagrams (from 2.7 to 1.0 mm anterior to bregma) from the rat brain atlas of Paxinos & Watson (1997) by direct visualization of slides using a light microscope. Schematics were subsequently assembled in Adobe Photoshop CS2.

Dual immunofluorescence

For immunofluorescence, sections were visualized using a confocal microscope (Zeiss LSM 510 Meta; Carl Zeiss Inc., Thornwood, NY, USA). *Z*-stacks from areas with dual labeling were collected and analyzed; single optical planes were analyzed individually for distribution and co-localization of the two markers throughout the thickness of the section. The data presented represent projections of six to nine single optical planes except for dual fluorescence in the NTS and CB1R and MAP2 pictures, for which a single plane from the *z*-stack is shown. Digital images were obtained and imported using the LSM 5 image browser. Figures were assembled and adjusted for brightness and contrast in Adobe Photoshop CS2.

Electron microscopy

For ultrastructural analysis, at least 15 grids containing four to eight thin sections (74 nm of thickness) each were collected from at least three plastic-embedded sections of the mid-ventral shell of the Acb from each animal. Thin sections were viewed using a Morgagni 268 digital electron microscope (FEI Company, Hillsboro, OR, USA), initially at low magnification to ensure that background labeling in the neuropil, deemed spurious, was not commonly encountered, then at higher magnification to verify adequate cellular morphology. For quantification, electron micrographs from thin sections of three animals that showed optimal preservation of ultrastructural morphology were taken at different magnifications, usually at 11 000× and then at 14 000× to 22 000× for better resolution of the structures analyzed. Figures presented were assembled and adjusted for brightness and contrast in Adobe Photoshop CS2. Selective gold–silver-labeled profiles were identified by the presence of at least two gold particles within a cellular compartment. The criterion of a minimum of two gold particles as indicative of positive immunolabeling is based on the fact that one gold particle could occasionally be found in profiles known to lack CB1R or NET immunoreactivity, such as myelin and blood vessels. Immunoperoxidase labeling was regarded as positive when the electron-dense precipitate in individual profiles was considerably greater than that seen in other morphologically similar profiles in the neuropil. The cellular elements were identified based on the description of Peters *et al.* (1991). Somata contained a nucleus, Golgi apparatus and smooth endoplasmic reticulum. Proximal dendrites contained endoplasmic reticulum, were postsynaptic to axon terminals and were > 0.7 μm in diameter. A terminal was considered to form a synapse if it showed a junctional complex, a restricted zone of parallel membranes with slight enlargement of the intercellular space and/or associated with postsynaptic thickening. Asymmetric synapses were identified by thick postsynaptic densities (Gray's type I); in contrast, symmetric synapses had thin densities (Gray's type II) both pre- and postsynaptically. The term 'undefined' synaptic contact was used to denote parallel membrane association of an axon terminal plasma membrane juxtaposed to that of a dendrite or soma which lacked recognizable membrane specializations in the plane of section analyzed, and with no intervening glial processes. The term 'apposition' is also used to denote close parallel membrane associations of axon terminals with other axon terminals and/or dendrites which lacked recognizable specializations but were otherwise not separated by glial processes.

Results

WIN 55,212-2 altered the expression of adrenergic receptors in the Acb

The influence of a cannabinoid agonist on adrenergic receptor expression in the Acb was assessed by Western blot analysis of protein extracts that were obtained from the Acb of animals that received either an acute systemic injection of WIN 55,212-2, repeated

systemic injections of WIN 55,212-2 or repeated systemic injections of WIN 55,212-2 followed by a period of abstinence. The region targeted for tissue dissection included the area medial to the anterior commissure (shell and medial core). As reported by others (Rudoy & Van Bockstaele, 2007), protein extracts indicative of α2A-AR could be identified at ∼45 kDa while proteins indicative of β1-AR migrated to ∼65 kDa.

Several studies have reported that CB1R agonists have biphasic effects on behavior according to the dose used, with lower doses stimulating locomotion and higher doses inhibiting it (Rodriguez de Fonseca *et al.*, 1998; Drews *et al.*, 2005). Cannabinoids have also been shown to have anxiolytic and anxiogenic effects on animals (Witkin *et al.*, 2005). For the dose–response study, a one-way ANOVA demonstrated a significant difference among treatment groups in β1-AR protein expression ($P = 0.02$; $F_{3,12} = 10.833$) and *post hoc* comparison tests revealed that acute administration of WIN 55,212-2 induced a decrease in the expression of β1-AR at concentrations of 1.0 and 3.0 mg/kg ($P < 0.05$) when comparing to vehicle-treated animals (Fig. 3A). Conversely, one-way ANOVA revealed no significant difference in α2A-AR protein expression ($P = 0.271$; $F_{3,14} = 1.49$), demonstrating that none of the concentrations used had an effect on α2A-AR protein levels in the Acb with an acute injection (Fig. 3A). To investigate the effects of repeated administration of WIN 55,212-2, the 3.0 mg/kg concentration was used as it has also been shown that this concentration, but not 1.0 mg/kg, increases extracellular NE in the PFC (Oropeza *et al.*, 2005). In addition, 3.0 mg/kg has been shown to induce c-fos expression in the NTS (Jelsing *et al.*, 2009). Worthy of note, the high dose used (7.0 mg/kg) had very pronounced sedative effect on the animals, making this dose unsuitable for future studies.

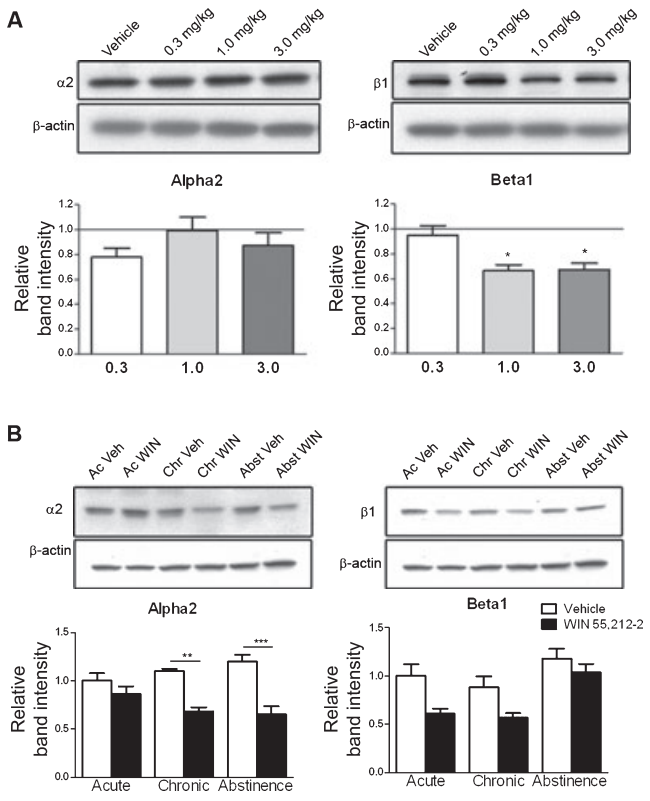

FIG. 3. Western blot for α2A and β1 adrenergic receptors (α2A- and β1-AR) from the Acb following WIN 55,212-2 treatment. Bands shown are representative of one sample from one animal of each group. (A) Dose–response study showing that acute administration of WIN 55,212-2 decreased the levels of β1-AR in the Acb at 1.0 and 3.0 mg/kg (*$P < 0.05$). None of the doses used had an effect on the levels of α2A-AR. (B) Western blot for α2A- and β1-AR in protein extracts from the Acb of rats administered WIN 55,212-2 (3.0 mg/kg) or vehicle, acutely (one injection) or chronically (7 days) and killed 40–45 min or 7 days (Chr+Abst group) after the last injection. α2A-AR expression was not altered by acute treatment with WIN 55,212-2. However, after chronic treatment there was a significant (**$P < 0.01$) decrease in the expression of α2A-AR and this decrease persisted in the absence of the drug for 7 days (Chr+Abst group; ***$P < 0.001$). Two-way ANOVA shows that β1-AR expression was significantly reduced after treatment with WIN 55,212-2 when compared to vehicle-treated animals. Data are presented as mean (+SEM) of change in band intensity normalized to values for vehicle-treated animals, with acute vehicle-treated animals set at 1.

To assess the effects of repeated administration of WIN 55,212-2 in α2A-AR and β1-AR protein expression a two-way ANOVA on the interaction between drug treatment (vehicle and drug) and treatment duration (acute, chronic and abstinence) was conducted (Fig. 3B). With respect to the effects in α2A-AR expression, the analysis revealed a significant interaction between the two factors ($P = 0.03$, $F_{2,26} = 4.103$). Therefore, a simple effects tests comparing vehicle- and drug-treated animals were conducted for the acute, chronic and abstinence conditions. A Bonferronni correction was applied. No differences in α2A-AR expression were observed with an acute injection of WIN 55,212-2 (3.0 mg/kg). However, the mean difference observed in the chronic condition (mean difference 0.42) was significant ($P < 0.01$; t (5) = 7.09). Similar effects were observed for the abstinence condition [mean difference 0.54; $P < 0.001$; t (11) = 4.87]. This shows that repeated treatment with WIN 55,212-2 (3.0 mg/kg) for 7 days (chronic group) significantly decrease the expression of α2A-AR and that this effect persisted over time as α2A-AR expression levels remained below control levels in the abstinence group. With respect to the effects in β1-AR protein expression, the analysis revealed a significant effect of drug treatment ($P < 0.001$; $F_{1,32} = 15.32$) and treatment duration ($P < 0.001$; $F_{2,32} = 10.67$). The effect of treatment condition suggested that subjects given WIN 55,212-2 showed a significantly decrease in β1-AR expression comparing to vehicle-treated animals. However, no interaction between the two factors was found ($P = 0.353$; $F_{2,21} = 1.076$).

Two-way ANOVA revealed no significant interaction between α2A-AR ($P = 0.668$; $F_{2,16} = 0.414$) and β1-AR ($P = 0.29$; $F_{2,18} = 1.327$) protein expression in samples from the cerebellum, an area rich in CB1R and noradrenergic input (data not shown). No significant effect was observed with respect to NET expression after treatment with WIN 55,212-2 (3.0 mg/kg; $P = 0.466$; $F_{1,18} = 0.555$; supporting Fig. S5).

Topographic distribution of CB1R in Acb core and shell subregions

The Acb extends for ∼2.2 mm in the ventral striatum and is composed of a central 'core' and a peripheral and medially situated 'shell' subregion (Zahm, 1999; van Dongen *et al.*, 2008). To adequately distinguish the neuroanatomical boundaries of the core and shell subregions within the Acb, calbindin immunoreactivity was used as a marker to define these two subregions in adjacent coronal sections. As previously reported (Jongen-Relo *et al.*, 1994; Tan *et al.*, 1999), calbindin immunoreactivity was more prominent in the core and the overlying striatum where it often appeared in cell bodies (Fig. 4B). Our data are consistent with these reports, as calbindin immunoreactivity appeared prominently in the Acb core where peroxidase-labeled cell bodies could be identified immediately adjacent to the anterior commissure and approaching the lateral ventricle dorsally. The

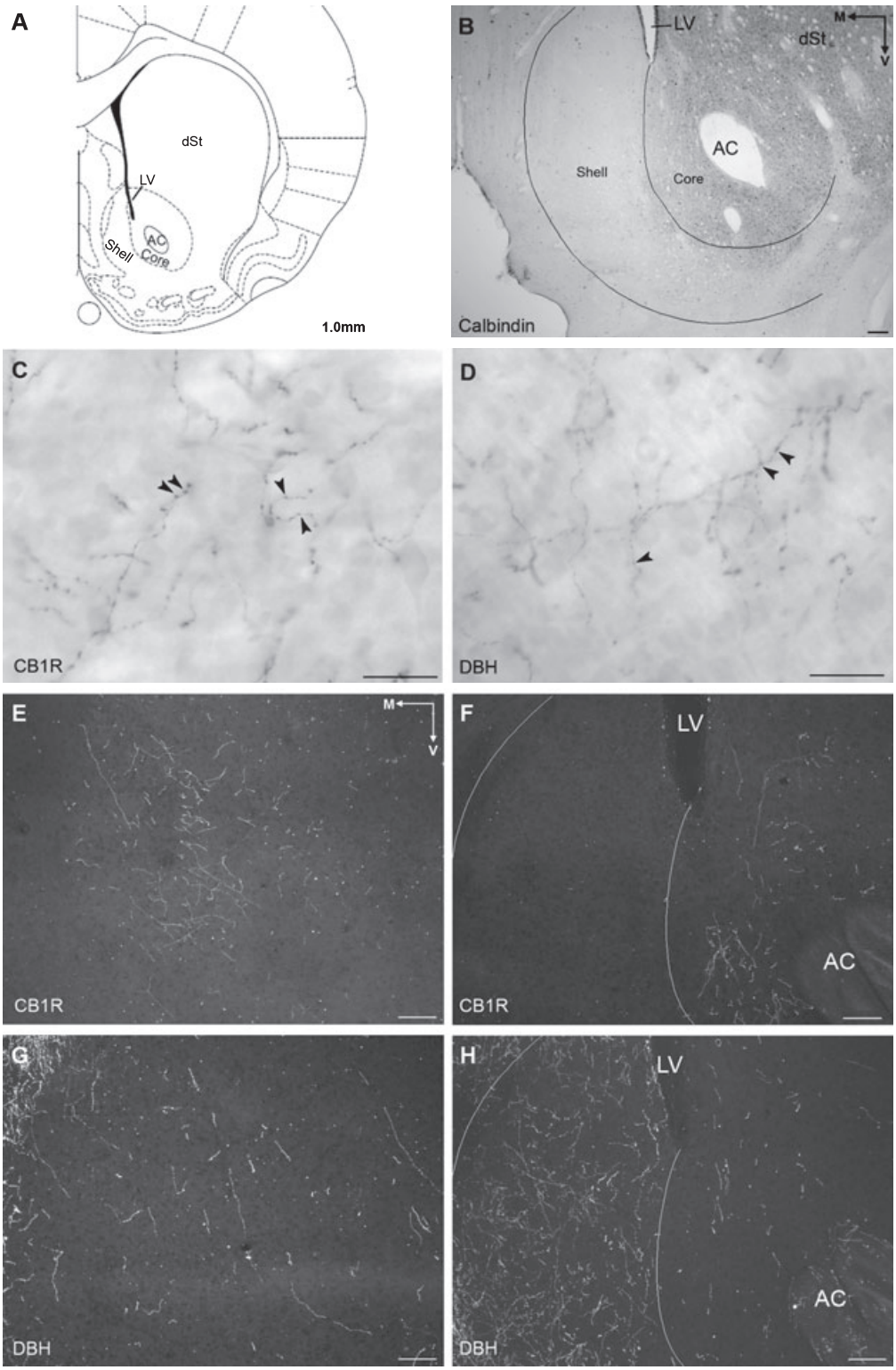

FIG. 4. (A) Diagram of a coronal section of rat forebrain adapted from the rat brain atlas of Paxinos & Watson (1997) showing subregions of the Acb in the ventral striatum. The core subregion of the Acb surrounds the anterior commissure (AC) whereas the shell subregion is situated medial and ventral to the lateral ventricle (LV). (B) Brightfield photomicrograph of calbindin immunoreactivity in a coronal section of rat brain at an equivalent level to that shown in panel (A). Calbindin immunoreactivity is more intense in the core and dorsal striatum (dSt), with almost no labeling in the shell. (C and D) Brightfield photomicrographs, from the shell of the Acb at ~1.7 mm anterior to bregma, of CB1R and DBH-ir, respectively. High magnification of CB1R and DBH-ir shows tortuous and beaded (arrowheads) processes. (E and F) Darkfield photomicrographs of CB1R immunoreactivity at two different levels of the Acb. CB1R-ir is seen (E) in the shell at mid-levels, ~0.7 mm anterior to bregma and (F) in the core at more caudal levels (1.0 mm anterior to bregma). (F) At this level, CB1R immunoreactivity is almost completely absent from the dorsal shell. (G and H) Darkfield photomicrographs showing DBH immunoreactivity at the same level as CB1R immunoreactivity in E and F, respectively. (G) Some DBH immunoreactivity is seen at mid-levels of the shell and (H) intense DBH immunoreactivity is seen in the shell at caudal levels. M, medial; V, ventral. Scale bar, 100 μm (B and E–H), 25 μm (C and D).

distribution of calbindin immunoreactivity, along with the anterior commissure and lateral ventricle, were used as references to identify the level of Acb and its subregions when analyzing the distribution of CB1R and DBH (Fig. 4A and B). The rostrocaudal segment of the Acb was systematically categorized into three levels for the purpose of the analysis: rostral (from 2.7 to 1.7 mm anterior to bregma), middle (from 1.7 to 1.0 mm anterior to bregma) and caudal (from 1.0 to 0.6 mm anterior to bregma), coordinates according to the rat brain atlas of Paxinos & Watson (1997).

Localization of CB1R in the Acb was consistent with previous reports (Robbe *et al.*, 2001; Pickel *et al.*, 2004; Kearn *et al.*, 2005). Immunoperoxidase and immunofluorescence labeling of CB1R was identified in long, beaded processes (Figs 4C, and 5A and B) consistent with axonal profiles and punctate deposits that were more consistent with a postsynaptic distribution (Fig. 5A). For simplicity, only CB1R processes are represented on the schematic illustrations (Fig. 6). CB1R-immunoreactive (-ir) processes were found throughout the rostrocaudal extent of the Acb but with a differential distribution within the shell and core subregions. CB1R-ir shifted from dorsal to ventral aspects of the shell with caudal progression through the Acb. However, in the caudal third division of the Acb, CB1R-ir was more prominent within the Acb core subregion (up to +1.0 mm from bregma), with little immunoreactivity in the shell (Fig. 4F). Clusters of CB1R-ir processes were particularly evident in the mid-ventral shell and in the core at caudal levels (Figs 4E and F, and 5B). CB1R labeling was seen in long processes running either medially or ventrally. Although not depicted on the schematic illustrations, CB1R was also seen in profiles consistent with somatodendritic structures (Fig. 5A) as reported by others (Pickel *et al.*, 2004; Kearn *et al.*, 2005; Villares, 2007). To confirm the somatodendritic localization of CB1R in this region, dual immunofluorescence of CB1R and the somatodendritic marker MAP2 showed double labeling, indicating that CB1R was also present postsynaptically (Fig. 5E).

At the ultrastructral level, using the immunogold–silver detection method, CB1R was identified both pre- (Fig. 7A) and postsynaptically (Fig. 7B) in cellular profiles. Of 342 CB1R-ir cellular profiles examined, 55% (189/342) were found in axon terminals and 45% (153/342) in dendrites. Pickel *et al.* (2004) reported similar values: 59% in terminals and 41% in dendrites. Similar values were obtained when CB1R was visualized using immunoperoxidase detection. Immunocytochemical labeling for CB1R-ir was identified along the plasma membrane of axon terminals as well as within the axoplasm (Fig. 7). Axon terminals that exhibited CB1R-ir were unmyelinated and contained synaptic vesicles that were heterogeneous in nature. CB1R-ir dendrites contained mitochondria and endoplasmic reticulum and were postsynaptic, mainly to unlabeled terminals. Of the axon terminals exhibiting CB1R-ir, synaptic specializations were characterized as symmetric or asymmetric. Semiquantitative analysis showed that, out of 189 profiles counted, 17% (32/189) formed symmetric synapses while 20% (37/189) formed asymmetric synapses (Fig. 7A). The remaining profiles did not form sufficiently clearly recognizable synaptic specializations in the plane of section analyzed to be accurately classified.

Topographic distribution of DBH in Acb core and shell subregions

Although distributed throughout the entire rostrocaudal extent of the Acb, DBH-ir fibers also showed a topographic distribution (Fig. 4 and 6). DBH-ir was found in both the shell and core of the Acb except at more caudal levels (+1.0 to +0.7 mm from bregma), where DBH-ir was found mainly in the shell (Fig. 4H). This level corresponded to the area of the Acb with the highest density of DBH-ir, where abundant, beaded and tortuous DBH-ir fibers were seen. The density of DBH-ir fibers decreased towards more rostral levels, with few fibers being detected at the most rostral level (2.7 mm anterior to bregma). Regions of high overlap between DBH-ir and CB1R-ir included the ventromedial shell at mid-levels of the Acb (Fig. 6, panels 1.7 and 1.6 mm).

Ultrastructural analysis of noradrenergic terminals was also assessed by electron microscopy. NET was used as a marker to detect noradrenergic axon terminals and did not compromise the ultrastructural preservation of the neuropil. In order to assure that NET labeled the same profiles as DBH, dual immunofluorescence was performed; co-localization of the two markers in the same profiles occurred (supporting Fig. S4). At the ultrastructural level, NET was detected only in axon terminals. The peroxidase reaction resulted in a difuse labeling within the terminals, with more intense labeling adjacent to the plasma membrane (arrows in Fig. 7), while immunogold–silver particles were found mainly in the cytoplasm, as reported by Miner *et al.* (2003) in the PFC. Detection of NET with immunogold–silver particles allowed better characterization of the synaptic specialization of these axon terminals in 31% of the terminals analyzed (47/153). NET was found to form mainly symmetric synapses (31 of 47; 66%), in accordance with studies in the PFC (Miner *et al.*, 2003), while asymmetric synapses were found in 34% (16/47).

Immunofluorescence microscopy showed that CB1R and DBH overlapped in both core and shell subregions of the Acb

Dual immunofluorescence for CB1R and DBH was conducted in the same section of tissue to determine whether noradrenergic afferents exhibit CB1R immunoreactivity. Both CB1R- and DBH immunoreactivity were found in beaded and tortuous processes (Fig. 5). The beaded morphology was more evident within the DBH-ir fibers (Fig. 5B and C). The distribution of CB1R- and DBH immunoreactivity in the Acb was in concordance with the data obtained from single labeling described above. Although CB1R immunoreactivity was often found in areas containing noradrenergic fibers, rarely were noradrenergic fibers positive for CB1R. However, in these areas of overlap, CB1R- and DBH immunoreactivity appeared to converge on common structures as the processes appeared to delineate cell bodies of neurons in the Acb (double arrows in Fig. 5B), suggesting that noradrenergic fibers and fibers containing CB1R may be converging on common neurons.

Noradrenergic afferents to the shell of the Acb showed a low frequency of co-existence with CB1R

The dual immunofluorescence data suggested multiple sites of interaction between CB1R and noradrenergic afferents that could only be fully resolved using ultrastructural analysis. The selection of the mid-ventral shell of the Acb for EM analysis was based on the light-microscopic data showing significant overlap in this area (Fig. 6). NET was detected using immunoperoxidase while CB1R was localized using immunogold–silver deposits (Fig. 7). In the area sampled, CB1R and noradrenergic terminals were found to physically interact in two ways. Some noradrenergic terminals were found to have CB1R and some were found to be apposed to unlabeled profiles containing CB1R. More specifically, 7.7% (9/113) of all NET-ir axon terminals contained CB1R immunogold–silver particles, while 4.8% (9/189) of all CB1R-containing axon terminals were found in NET-ir

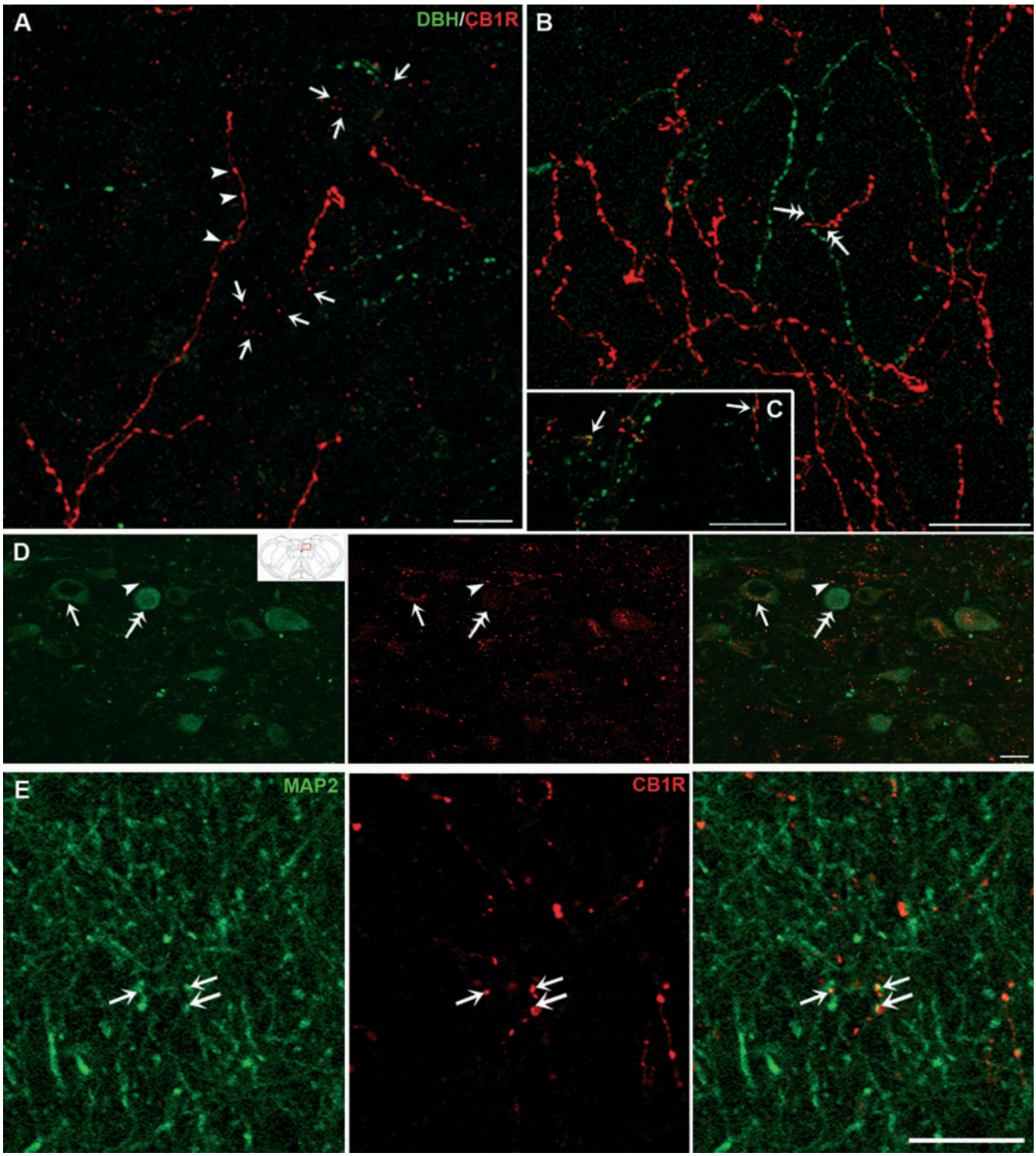

FIG. 5. Confocal fluorescence photomicrographs showing dual-labeling for CB1R and DBH in coronal sections of (A–C) the Acb and (D) the NTS, and (E) CB1R and MAP2 in the Acb. CB1R was detected using a rhodamine isothiocyanate (red)-conjugated secondary antisera and DBH and MAP2 were detected using a fluorescein isothiocyanate (green)-conjugated secondary antisera. Inset is a schematic diagram adapted from the rat brain atlas of Paxinos & Watson (1997) showing the level (14.08 mm posterior to bregma) at which the photomicrograph was taken. (A–C) CB1R and DBH immunoreactivity are frequently seen in the same field throughout the Acb. Both immunoreactivities show beaded processes resembling axonal structures (arrowheads in A) and punctate labeling consistent with postsynaptic profiles (arrows in A). Some co-localization of the two markers (arrows in C) can be seen. In addition, independently labeled fibers appear to converge on common structures (double arrows in B). (D) CB1R immunoreactivity is associated with DBH-labeled neurons (arrow) as well as unlabeled neurons (arrowhead) in the NTS. Some of the DBH-labeled neurons lack CB1 immunoreactivity (double arrows). (E) Localization of CB1R in somatodendritic profiles labeled with MAP2 (arrows). Scale bars, 20 μm.

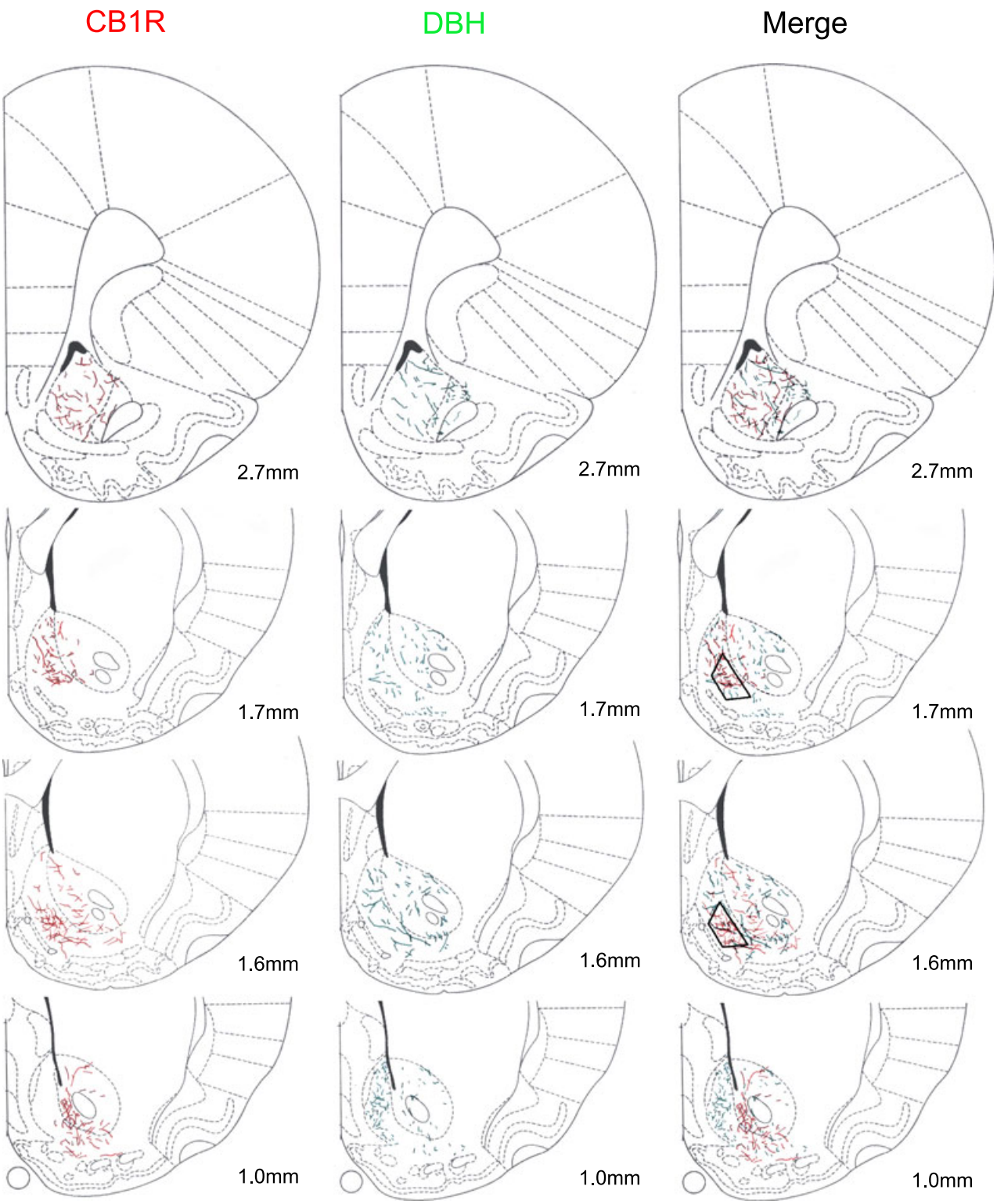

FIG. 6. Distribution of CB1R and DBH immunoreactivities along the extent of the Acb shown in schematics adapted from the rat brain atlas of Paxinos & Watson (1997). Distances shown represent location anterior to bregma. CB1R immunoreactivity is depicted in schematics on the left while DBH immunoreactivity is shown in schematics in the middle column. CB1R immunoreactivity was found diffusely in the core and in the shell subregions in the rostral third area of the Acb. At mid-levels (1.7–1.0 mm), CB1R was found mainly in the shell and there was a rostrocaudal shift in CB1R immunoreactivity from the dorsal shell to the ventral shell. In the caudal third of the Acb (up to 1.0 mm), CB1R immunoreactivity was found almost exclusively in the core. DBH immunoreactivity was found diffusely in the shell and core subregions, with increased density as the nucleus progressed caudally. In the caudal third of the Acb (up to 1.0 mm), DBH immunoreactivity was very intense in the shell and less so in the core. Trapezoids in the right column indicate the region sampled for ultrastructural analysis of CB1R and DBH distribution.

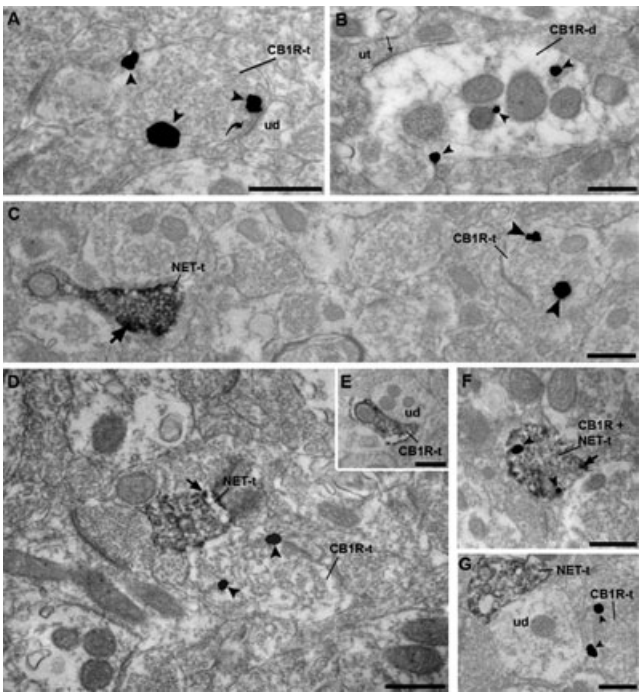

FIG. 7. Electron photomicrographs from the Acb shell subregion showing immunogold–silver labeling (arrowheads) for CB1R and immunoperoxidase labeling for NET. Irrespective of whether the immunolabeling was in (A) an axon terminal or (B) a dendrite, immunogold–silver particles for CB1R could be detected within the cytoplasm as well as associated with the plasma membrane. (A) Example of immunogold–silver labeling for CB1R in an axon terminal (CB1R-t) forming an asymmetric, excitatory-type synapse (curved arrow) with an unlabeled dendrite (ud). (B) CB1R immunolabeling is present in a dendrite (CB1R-d) that receives a symmetric, inhibitory-type synapse (thin arrow) from an unlabeled terminal (ut). (C) Dual localization of NET and CB1R using immunoperoxidase detection for NET and gold–silver labeling for CB1R. NET can be identified in an axon terminal by the presence of a diffuse peroxidase precipitate with intense immunoreactivity along the plasma membrane (thick black arrow). The immunoperoxidase-labeled NET axon terminal (NET-t) is found in the same field as a CB1R-t that is labeled with gold–silver particles (arrowheads). (D) A NET-t is apposed to a CB1R-t labeled with immunogold–silver. (E) Example of reverse labeling using immunoperoxidase for CB1R which is apposed to an unlabeled dendrite (ud). (F) An example of an axon terminal that exhibits labeling for both CB1R and NET (CB1R + NET-t). (G) A NET-t exhibiting immunoperoxidase labeling and a CB1R-t converging onto the same unlabeled dendrite (ud). Scale bars, 500 nm.

axon terminals (Fig. 7F). With respect to the apposed labeling, 6.2% (7/113) of all NET-ir axon terminals were apposed to profiles containing CB1R immunogold–silver particles (Fig. 7D). Conversely, 1.6% of all CB1R-containing axon terminals were apposed to NET-ir axon terminals, while 2.6% of all CB1R-containing dendrites were apposed to NET-ir axon terminals. In regions of apposition, no synaptic specialization of the CB1R-containing terminals was recognizable in the cross-section analyzed.

CB1R were located in noradrenergic neurons in the NTS

As the cannabinoid agonist was administered systemically, the effects of WIN 55,212-2 on the expression of AR in the Acb could also be due to its actions on CB1R located in noradrenergic nuclei projecting to the Acb, i.e. the NTS. To assess this, dual immunofluorescence for CB1R and DBH was performed in tissue sections containing the NTS. DBH immunoreactivity was found diffusely in cell bodies as well as in processes resembling dendrites (Fig. 5D). CB1R immunoreactivity exhibited a punctate distribution and co-localized in the cytoplasm of noradrenergic neurons (positive for DBH) as well as non-noradrenergic neurons (lacking DBH-ir). Some of the DBH-labeled neurons lacked CB1R-ir.

Discussion

The present study demonstrates that systemic administration of a cannabinoid agonist alters the expression of ARs in a key limbic forebrain region related to motivated behaviors. Light and ultrastructural microscopy studies indicate several potential cellular sites for interaction between the two systems that include co-existence in common axon terminals, serial modulation by convergence of separately labeled axon terminals on common postsynaptic targets and indirect effects on noradrenergic brainstem perikarya that provide afferent input to the Acb.

Methodological considerations

The present study analyzed the expression of AR in the Acb following treatment with WIN 55,212-2 or vehicle. The Acb can be divided into core and shell subregions. At more rostral levels, the two regions can be easily microdissected but at more caudal levels the core subregion completely surrounds the anterior commissure while the shell subregion surrounds it ventrally. To avoid dissecting the anterior commissure we oriented our micropunches to target the Acb medial to the anterior commissure, leaving out the core that sits lateral to it and part of the ventrolateral shell from the dissection. As micropunches of the Acb were used for the quantification of the ARs, the exact area where these changes occurred (shell vs. core subregions, rostral vs. caudal) cannot be established. Also, whether the changes observed are due to a decrease in both pre- and postsynaptic receptors cannot be defined.

A potential limitation known to be associated with the pre-embedding immunolabeling technique is penetration of immunoreagents in thick Vibratome sections (Chan *et al.*, 1990). To circumvent this possibility, analysis of ultrathin sections was carried out exclusively on sections near the tissue–plastic interface where penetration is maximal. Limitations associated with the specificity of immunogold labeling were overcome by quantifying only the profiles containing two or more immunogold–silver particles. This may lead to an underestimation of actual cellular relationships. However, this approach minimized the reporting of potential spurious gold labeling.

AR changes in the Acb following CB1R agonist treatment

To our knowledge, we are the first to report a change in adrenergic receptor expression in the Acb following exposure to systemic administration of the synthetic cannabinoid agonist WIN 55,212-2. Our results demonstrate a decrease in β1- and α2A-AR protein expression in the Acb following acute and/or chronic exposure. A decrease in protein expression levels may be related to downregulation of the receptor as adrenergic receptors, which belong to the G protein-coupled receptor (GPCR) superfamily, are known to desensitize, internalize and downregulate their expression following binding of an agonist (Heck & Bylund, 1997; Dunigan *et al.*, 2002). Because desensitization does not seem to depend on protein degradation (as removal of agonist rapidly restores receptor function; Hein & Kobilka, 1995), no differences in total receptor protein would be expected during desensitization. In contrast, downregulation of

GPCRs can be defined as a loss of total cellular binding activity or decrease in receptor density (Barturen & Garcia-Sevilla, 1992; Hein & Kobilka, 1995; Heck & Bylund, 1997). Mechanisms for downregulation may include protein degradation, destabilization of the receptor mRNA or repression of gene transcription.

We have previously reported that acute and chronic systemic administration of WIN 55,212-2 is capable of increasing NE release in the PFC with concomitant activation of c-fos activation in brainstem noradrenergic neurons (Oropeza *et al.*, 2005; Page *et al.*, 2007). In addition, others have shown that WIN 55,212-2 (3.0 mg/kg) is able to induce c-fos expression in the NTS (Jelsing *et al.*, 2009). It is tempting to speculate that the downregulation of AR in the Acb following WIN 55,212-2 may occur due to an increase in NE release in the Acb. The fact that NET expression in the Acb is not affected by WIN 55,212-2 administration suggests that the reuptake of NE by this transporter remains constant although binding tests should be performed to confirm this. We have recently described a decrease in β1-AR levels in the PFC after chronic treatment with WIN 55,212-2, with no changes in the levels of α2A-AR (Reyes *et al.*, 2009). The distinct effect of WIN 55,212-2 on the levels of ARs in the PFC and Acb may account for the anatomical and functional differences between the two areas. Anatomically, the PFC receives its noradrenergic input solely from the LC while the Acb is innervated mainly by the NTS (Delfs *et al.*, 1998; Olson *et al.*, 2006). The present study, therefore, by assessing noradrenergic afferents to the Acb, provides information regarding the interaction of the cannabinoid system with limbic-forebrain projections originating specifically from the NTS. Also, the subcellular localization of the AR in the Acb is not known but they are found to be both pre- and postsynaptic in other brain regions such as the PFC (MacDonald *et al.*, 1997; Ramos & Arnsten, 2007; Wang *et al.*, 2007). The localization of AR with CB1R is being analyzed and, based on previous studies showing preferential presynaptic localization of α2-AR (Flugge *et al.*, 2004), we hypothesize that axon terminals in the Acb expressing α2-AR will be apposed to terminals containing CB1R. Considering our localization of CB1R in dendrites and the known association of β1-AR receptors with the postsynaptic density protein in other brain regions (Strader *et al.*, 1983; Aoki *et al.*, 1987; Hu *et al.*, 2000), we also anticipate a potential co-localization of β1-AR and CB1R postsynaptically. It has been proposed that activation of CB1R can sequester G proteins, making them unavailable for other GPCRs such as α2-AR and somatostatin receptors (Vasquez & Lewis, 1999). Whether disruption of this GPCR signaling can ultimately lead to their downregulation has not been addressed yet. Activation of CB1R is also known to lead to changes in membrane potential and to alter the levels of intracellular cAMP (Demuth & Molleman, 2006). cAMP can initiate intracellular pathways that can lead to inhibition of AR synthesis or to destabilization of AR mRNA, contributing to downregulation of the receptor (Kirigiti *et al.*, 2001; Dunigan *et al.*, 2002). In addition, stimulation of CB1R activates protein kinases that could participate in the regulation of gene expression (Piomelli, 2003).

CB1R and DBH were topographically distributed within the Acb

Our data are in agreement with others' with regard to the presence of noradrenergic terminals and CB1R immunoreactivity in the Acb (Berridge *et al.*, 1997; Delfs *et al.*, 1998; Tsou *et al.*, 1998; Robbe *et al.*, 2001). However, the present study adds a detailed analysis of the distribution of CB1R immunoreactivity not provided in these studies. Robbe *et al.* (2001) identified CB1R immunoreactivity in large, poorly branched fibers exhibiting intensely immunostained varicosities that were localized mostly in the core subregion of the Acb. We report the same type of immunostaining for CB1R but we provide new data showing that CB1R is also found in the shell subregion. Our analysis shows that CB1R immunoreactivity is not uniform throughout the Acb. CB1R immunoreactivity is mainly found in the core in the caudal third of the Acb and is found in the remaining two-thirds of the nucleus in the shell subregion. Hence, CB1R immunoreactivity seems to be more abundant in the shell. Careful analysis by light microscopy of CB1R immunoreactivity in both the core and the shell subregions did not reveal major differences in the immunostaining pattern between the subregions, suggesting that CB1R may function similarly in both the shell and core. The distribution of DBH-ir in the Acb presented in this study is in agreement with previous studies (Berridge *et al.*, 1997; Delfs *et al.*, 1998). More specifically, DBH-ir was reported to be more evident in the shell at caudal levels but it was also found at more rostral levels, both in the shell and in the core.

In summary, our mapping of CB1R and DBH immunoreactivity in the Acb shows an interesting topographic distribution of the two markers. CB1R and DBH were shown to have an uneven distribution throughout the nucleus. This fact may be relevant for the anatomic and functional heterogeneity proposed for the Acb (Zahm, 1999). Anatomical and behavioral studies support a rostrocaudal gradient for appetitive vs. aversive behaviors (Reynolds & Berridge, 2001, 2002, 2003). These studies suggest that the rostral shell is important for appetitive/hedonic behaviors whereas the caudal shell is important for aversive/fear behaviors, and that GABAergic and glutamatergic transmission (through $GABA_A$ and AMPA receptors) is involved. Modulation of GABAergic and glutamatergic transmission in the intermediate shell produces combined positive and negative motivational effects. Whether the overlapping region of DBH and CB1R immunoreactivities described in the present study correlates with these behaviors cannot be established. However, our ultrastructural analysis of the middle third of the shell subregion localized CB1R to terminals forming symmetric (inhibitory) and asymmetric (excitatory) synapses, suggesting that activation of CB1R can modulate inhibitory and excitatory input in the Acb and therefore modulate behavior. In addition, previous studies have shown that cannabinoids are able to inhibit glutamate and GABA transmission in the Acb (Hoffman & Lupica, 2001; Manzoni & Bockaert, 2001; Robbe *et al.*, 2001; Hoffman *et al.*, 2003), mainly through a presynaptic mechanism. Future studies should also address whether the presence of noradrenergic fibers in this specific region is important for the modulation of the abovementioned behaviors.

Subcellular localization of CB1R in the Acb

The CB1R subcellular distribution in the shell of the Acb analyzed in the present study by electron microscopy is agreement with previous studies but also shows some differences (Pickel *et al.*, 2004; Matyas *et al.*, 2006). Discrepancies in anatomical studies may arise from multiple factors. For example, the region of the Acb analyzed may differ from study to study. As shown in the present study, the distribution of both CB1R and noradrenergic fibers varies considerably throughout the nucleus and sampling differences between laboratories may lead to different results. In the present study, the area selected for ultrastructural analysis was restricted to the mid-ventral shell due to the higher incidence of overlap between CB1R and DBH immunoreactivity observed by light and fluorescence

microscopy. In addition, different criteria were used to quantify profiles that exhibited CB1R immunoreactivity. In the present study, only profiles containing two or more gold particles were included in the semi-quantitative analysis whereas other groups (Pickel *et al.*, 2004) considered single immunogold–silver profiles as indicative of positive labeling for CB1R. Finally, another difference relates to the type of synapses formed by terminals containing CB1R. Matyas *et al.* (2006) showed that all single-labeled CB1R-containing axon terminals and dual-labeled CB1R and GABA axon terminals formed exclusively symmetric synapses. On the other hand, Pickel *et al.* (2004) reported that 42% of the CB1R-labeled axon terminals formed asymmetric synapses while only 7% formed symmetric synapses. In the present study, a similar number of terminals formed symmetric and asymmetric synapses, although > 60% of the profiles exhibited synaptic specifications that could not be unequivocally established in the plane of section analyzed. Nevertheless, as mentioned before, cannabinoids have been found to affect both glutamate and GABA transmission in the Acb (Manzoni & Bockaert, 2001; Robbe *et al.*, 2001). The localization of CB1R in terminals forming symmetric and asymmetric synapses in the present study is consistent with this.

As reported by Pickel *et al.* (2004), the present study shows immunolabeling for CB1R in somatodendritc profiles in the Acb. This is an interesting finding as cannabinoid actions are thought to be mainly presynaptic. However, there is evidence for self-inhibition of cortical interneurons by cannabinoids in an autocrine manner, whereby cannabinoids are synthesized postsynaptically and activate nearby CB1R (Piomelli, 2003; Bacci *et al.*, 2004). Moreover, the fact that fatty acid amide hydrolase (one of the enzymes responsible for degradation of endocannabinoids) is located mainly in cell bodies and dendrites (Egertova *et al.*, 2003; Piomelli, 2003) may suggest that cannabinoids might be able to act postsynaptically. Nevertheless, whether CB1R located postsynaptically in the Acb are functional and activating intracellular pathways was not investigated in the present study and warrants further investigation.

Anatomical data show interaction between CB1R and DBH

Our anatomical data show multiple sites for interaction between the cannabinoid and noradrenergic systems in the Acb and the NTS (Fig. 8). CB1R was found in noradrenergic terminals, in unlabeled terminals apposed to noradrenergic terminals and in dendrites in the Acb as well as in noradrenergic and non-noradrenergic neurons of the NTS (Fig. 8, panel 1). Based on our anatomical data, we proposed four potential mechanisms by which WIN 55,212-2 is modulating AR expression. WIN 55,212-2 may be modulating the levels of AR directly by activating CB1R present in profiles that express AR (dendrites or axon terminals; Fig. 8, panel 2). WIN 55,212-2 can also act on CB1R present in noradrenergic terminals (Fig. 8, panel 2) modulating the release of NE. Continued agonist activation of AR by NE can lead to receptor downregulation (Hein & Kobilka, 1995; Heck & Bylund, 1997). A third intra-accumbal mechanism may account for modulation by WIN 55,212-2 of AR. The majority of CB1R was found in unlabeled profiles. The nature of these profiles is unknown, but activation of CB1R by WIN 55,212-2 may contribute to modulation of these profiles' transmission with consequent effects on noradrenergic terminals and profiles containing AR (Fig. 8, panel 3). Ultimately, WIN 55,212-2 may be acting on CB1R present in the NTS, increasing the noradrenergic input to the Acb (Fig. 8, panel 4). In fact, WIN 55,212-2 administration has been shown to induce c-fos activation in the NTS (Jelsing *et al.*, 2009). However, whether this

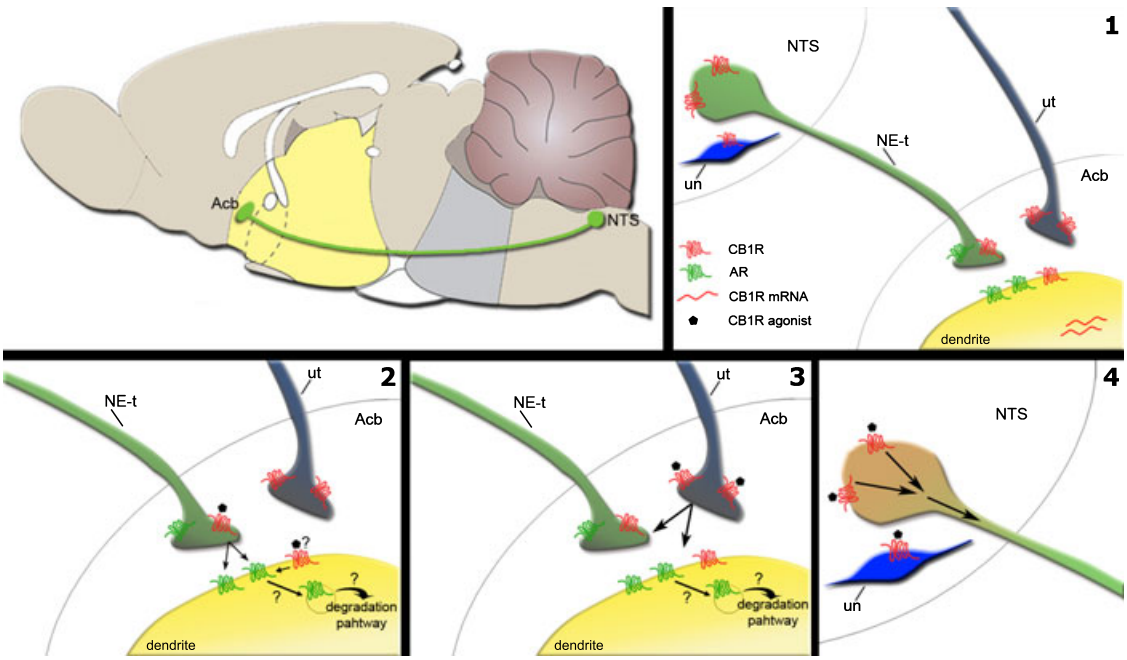

FIG. 8. Possible sites for modulation of noradrenergic transmission in the Acb by cannabinoids. (Top left panel). Schematic of a saggital rat brain showing the noradrenergic input to the Acb arising from the NTS. (1) The present study shows that, in the Acb, CB1R is found in noradrenergic terminals (NE-t), unlabeled terminals (ut) and in dendrites. CB1R is also present in somatodendritic profiles of noradrenergic neurons and unlabeled neurons (un) in the NTS. Adrenergic receptors (AR) can be found pre- and postsynaptically (MacDonald *et al.*, 1997; Ramos & Arnsten, 2007; Wang *et al.*, 2007). CB1R mRNA has been shown to be present in the Acb (Hohmann & Herkenham, 2000; Hurley *et al.*, 2003). We hypothesize that cannabinoids may modulate noradrenergic transmission in the shell of the Acb as follows. (2) Directly, through activation of CB1R present on noradrenergic terminals or dendrites. Whether dendritic CB1Rs are functional requires further studies. Nevertheless, if functionally active these receptors could influence adrenergic receptor expression. (3) Indirectly, through activation of CB1R in terminals apposed to noradrenergic terminals. (4) Indirectly, through activation of CB1R in the NTS neurons that send projections to the Acb.

neuronal activation increases NE release in the Acb remains to be elucidated.

Functional implications

Convergent studies in the literature suggest that cannabinoids may play a role in several neuropsychiatric disorders (Maldonado *et al.*, 2006; Leweke & Koethe, 2008; Moreira & Lutz, 2008) such as depression or schizophrenia. Interestingly, the CB1R antagonist rimonabant was withdrawn due to an unacceptably high incidence of neuropsychiatric side effects (Nissen *et al.*, 2008; Sanofi-Aventis), while CB1R agonists have been shown to alleviate depressive-like behaviors in animal models (Gobbi *et al.*, 2005; Hill & Gorzalka, 2005b). Moreover, Gobbi *et al.* (2005) showed that increased levels of anandamide evoked an increase in noradrenergic neuron activity in the LC. This is supported by previous work from our laboratory, showing that administration of a synthetic cannabinoid is able to activate the LC with increased levels of NE in the PFC (Oropeza *et al.*, 2005; Page *et al.*, 2007). The present study adds to these data, as the decrease in α2A-AR expression may account for the assumed increase in NE in the Acb, as α2A-AR seem to function as autoreceptors by inhibiting NE release from the presynaptic terminal (Kable *et al.*, 2000). In fact, local administration of α2-AR agonists in the Acb has been shown to reduce the efflux of NE measured by microdialysis, while administration of antagonists of α2-AR increased the release of NE (Aono *et al.*, 2007). Moreover, downregulation of β1-AR can be seen as a mechanism which is adaptive to an increase in synaptic NE. Although activation of α2-AR can decrease dopamine release in other brain regions such as the PFC and hippocampus (Guiard *et al.*, 2008; Jentsch *et al.*, 2008) this does not seem to be the case in the Acb. Ihalainen and colleagues have shown that administration of an α2-AR agonist would decrease dopamine in the Acb when administered systemically but not when it was locally administered (Ihalainen & Tanila, 2004). This supports the idea that α2-AR may be localized mainly in noradrenergic terminals in the Acb. Therefore, the impact of chronic WIN 55,212-2 on α2-AR levels in the Acb seems to be selective for noradrenergic terminals. As NE is an important target for the treatment of depression (Heninger *et al.*, 1996; Nutt, 2002), it is tempting to speculate that cannabinoids may impact mood- and motivation-related behaviors by activating limbic forebrain noradrenergic circuits.

Supporting Information

Additional supporting information may be found in the online version of this article:

Fig. S1. Specificity of the secondary antibody.

Fig. S2. Specificity of NET primary antibody.

Fig. S3. Specificity of β1-AR and α2A-AR antibodies.

Fig. S4. Confocal fluorescence photomicrographs showing dual-labeling for NET and DBH in coronal sections of the Acb. NET and DBH are co-localized to the same profiles.

Fig. S5. Results of western blot analysis for NET in the Acb showing that treatment with WIN 55,212-2 (3.0 mg/kg) does not affect NET expression.

Please note: As a service to our authors and readers, this journal provides supporting information supplied by the authors. Such materials are peer-reviewed and may be re-organized for online delivery, but are not copy-edited or typeset by Wiley-Blackwell. Technical support issues arising from supporting information (other than missing files) should be addressed to the authors.

Acknowledgements

This works was supported by PHS grant DA 020129. A.F.C. was supported by the Portuguese Foundation for Science and Technology (SFRH/BD/33236/2007).

Abbreviations

Acb, nucleus accumbens; AR, adrenergic receptor; BSA, bovine serum albumin; CB1R, cannabinoid receptor type 1; DBH, dopamine beta hydroxylase; GPCR, G protein-coupled receptor; -ir, -immunoreactive; LC, locus coeruleus; MAP2, microtubule associated protein 2; NE, norepinephrine; NET, norepinephrine transporter; NTS, nucleus of the solitary tract; PB, phosphate buffer; PFC, prefrontal cortex; TS, Tris saline buffer.

References

Anand, A. & Charney, D.S. (2000) Norepinephrine dysfunction in depression. *J. Clin. Psychiatry*, **61**(Suppl 10), 16–24.

Aoki, C., Joh, T.H. & Pickel, V.M. (1987) Ultrastructural localization of beta-adrenergic receptor-like immunoreactivity in the cortex and neostriatum of rat brain. *Brain Res.*, **437**, 264–282.

Aono, Y., Saigusa, T., Watanabe, S., Iwakami, T., Mizoguchi, N., Ikeda, H., Ishige, K., Tomiyama, K., Oi, Y., Ueda, K., Rausch, W.D., Waddington, J.L., Ito, Y., Koshikawa, N. & Cools, A.R. (2007) Role of alpha adrenoceptors in the nucleus accumbens in the control of accumbal noradrenaline efflux: a microdialysis study with freely moving rats. *J. Neural Transm.*, **114**, 1135–1142.

Aston-Jones, G., Chiang, C. & Alexinsky, T. (1991) Discharge of noradrenergic locus coeruleus neurons in behaving rats and monkeys suggests a role in vigilance. *Prog. Brain Res.*, **88**, 501–520.

Bacci, A., Huguenard, J.R. & Prince, D.A. (2004) Long-lasting self-inhibition of neocortical interneurons mediated by endocannabinoids. *Nature*, **431**, 312–316.

Barturen, F. & Garcia-Sevilla, J.A. (1992) Long term treatment with desipramine increases the turnover of alpha 2-adrenoceptors in the rat brain. *Mol. Pharmacol.*, **42**, 846–855.

Berridge, C.W., Stratford, T.L., Foote, S.L. & Kelley, A.E. (1997) Distribution of dopamine beta-hydroxylase-like immunoreactive fibers within the shell subregion of the nucleus accumbens. *Synapse*, **27**, 230–241.

Bodor, A.L., Katona, I., Nyiri, G., Mackie, K., Ledent, C., Hajos, N. & Freund, T.F. (2005) Endocannabinoid signaling in rat somatosensory cortex: laminar differences and involvement of specific interneuron types. *J. Neurosci.*, **25**, 6845–6856.

Callado, L.F., Meana, J.J., Grijalba, B., Pazos, A., Sastre, M. & Garcia-Sevilla, J.A. (1998) Selective increase of alpha2A-adrenoceptor agonist binding sites in brains of depressed suicide victims. *J. Neurochem.*, **70**, 1114–1123.

Chan, J., Aoki, C. & Pickel, V.M. (1990) Optimization of differential immunogold–silver and peroxidase labeling with maintenance of ultrastructure in brain sections before plastic embedding. *J. Neurosci. Methods*, **33**, 113–127.

Daniel, H. & Crepel, F. (2001) Control of ca(2+) influx by cannabinoid and metabotropic glutamate receptors in rat cerebellar cortex requires K(+) channels. *J. Physiol.*, **537**, 793–800.

De Paermentier, F., Cheetham, S.C., Crompton, M.R., Katona, C.L. & Horton, R.W. (1990) Brain beta-adrenoceptor binding sites in antidepressant-free depressed suicide victims. *Brain Res.*, **525**, 71–77.

De Paermentier, F., Cheetham, S.C., Crompton, M.R., Katona, C.L. & Horton, R.W. (1991) Brain beta-adrenoceptor binding sites in depressed suicide victims: effects of antidepressant treatment. *Psychopharmacology (Berl.)*, **105**, 283–288.

De Paermentier, F., Mauger, J.M., Lowther, S., Crompton, M.R., Katona, C.L. & Horton, R.W. (1997) Brain alpha-adrenoceptors in depressed suicides. *Brain Res.*, **757**, 60–68.

Delfs, J.M., Zhu, Y., Druhan, J.P. & Aston-Jones, G.S. (1998) Origin of noradrenergic afferents to the shell subregion of the nucleus accumbens: anterograde and retrograde tract-tracing studies in the rat. *Brain Res.*, **806**, 127–140.

Demuth, D.G. & Molleman, A. (2006) Cannabinoid signalling. *Life Sci.*, **78**, 549–563.

Di Chiara, G. (2002) Nucleus accumbens shell and core dopamine: differential role in behavior and addiction. *Behav. Brain Res.*, **137**, 75–114.

van Dongen, Y.C., Mailly, P., Thierry, A.M., Groenewegen, H.J. & Deniau, J.M. (2008) Three-dimensional organization of dendrites and local axon

collaterals of shell and core medium-sized spiny projection neurons of the rat nucleus accumbens. *Brain Struct. Funct.*, **213**, 129–147.
Drews, E., Schneider, M. & Koch, M. (2005) Effects of the cannabinoid receptor agonist WIN 55,212-2 on operant behavior and locomotor activity in rats. *Pharmacol. Biochem. Behav.*, **80**, 145–150.
Dunigan, C.D., Hoang, Q., Curran, P.K. & Fishman, P.H. (2002) Complexity of agonist- and cyclic AMP-mediated downregulation of the human beta 1-adrenergic receptor: role of internalization, degradation, and mRNA destabilization. *Biochemistry*, **41**, 8019–8030.
Egertova, M., Cravatt, B.F. & Elphick, M.R. (2003) Comparative analysis of fatty acid amide hydrolase and cb(1) cannabinoid receptor expression in the mouse brain: evidence of a widespread role for fatty acid amide hydrolase in regulation of endocannabinoid signaling. *Neuroscience*, **119**, 481–496.
Flugge, G., Van Kampen, M. & Mijnster, M.J. (2004) Perturbations in brain monoamine systems during stress. *Cell Tissue Res.*, **315**, 1–14.
Fox, K.M., Sterling, R.C. & Van Bockstaele, E.J. (2009) Cannabinoids and novelty investigation: influence of age and duration of exposure. *Behav. Brain Res.*, **196**, 248–253.
Gerdeman, G. & Lovinger, D.M. (2001) CB1 cannabinoid receptor inhibits synaptic release of glutamate in rat dorsolateral striatum. *J. Neurophysiol.*, **85**, 468–471.
Gobbi, G., Bambico, F.R., Mangieri, R., Bortolato, M., Campolongo, P., Solinas, M., Cassano, T., Morgese, M.G., Debonnel, G., Duranti, A., Tontini, A., Tarzia, G., Mor, M., Trezza, V., Goldberg, S.R., Cuomo, V. & Piomelli, D. (2005) Antidepressant-like activity and modulation of brain monoaminergic transmission by blockade of anandamide hydrolysis. *Proc. Natl. Acad. Sci. U S A*, **102**, 18620–18625.
Guiard, B.P., El Mansari, M. & Blier, P. (2008) Cross-talk between dopaminergic and noradrenergic systems in the rat ventral tegmental area, locus ceruleus, and dorsal hippocampus. *Mol. Pharmacol.*, **74**, 1463–1475.
Heck, D.A. & Bylund, D.B. (1997) Mechanism of down-regulation of alpha-2 adrenergic receptor subtypes. *J. Pharmacol. Exp. Ther.*, **282**, 1219–1227.
Hein, L. & Kobilka, B.K. (1995) Adrenergic receptor signal transduction and regulation. *Neuropharmacology*, **34**, 357–366.
Heninger, G.R., Delgado, P.L. & Charney, D.S. (1996) The revised monoamine theory of depression: a modulatory role for monoamines, based on new findings from monoamine depletion experiments in humans. *Pharmacopsychiatry*, **29**, 2–11.
Hill, M.N. & Gorzalka, B.B. (2005a) Is there a role for the endocannabinoid system in the etiology and treatment of melancholic depression? *Behav. Pharmacol.*, **16**, 333–352.
Hill, M.N. & Gorzalka, B.B. (2005b) Pharmacological enhancement of cannabinoid CB1 receptor activity elicits an antidepressant-like response in the rat forced swim test. *Eur. Neuropsychopharmacol.*, **15**, 593–599.
Hoffman, A.F. & Lupica, C.R. (2000) Mechanisms of cannabinoid inhibition of GABA(A) synaptic transmission in the hippocampus. *J. Neurosci.*, **20**, 2470–2479.
Hoffman, A.F. & Lupica, C.R. (2001) Direct actions of cannabinoids on synaptic transmission in the nucleus accumbens: a comparison with opioids. *J. Neurophysiol.*, **85**, 72–83.
Hoffman, A.F., Oz, M., Caulder, T. & Lupica, C.R. (2003) Functional tolerance and blockade of long-term depression at synapses in the nucleus accumbens after chronic cannabinoid exposure. *J. Neurosci.*, **23**, 4815–4820.
Hohmann, A.G. & Herkenham, M. (2000) Localization of cannabinoid CB(1) receptor mRNA in neuronal subpopulations of rat striatum: a double-label in situ hybridization study. *Synapse*, **37**, 71–80.
Hu, L.A., Tang, Y., Miller, W.E., Cong, M., Lau, A.G., Lefkowitz, R.J. & Hall, R.A. (2000) Beta 1-adrenergic receptor association with PSD-95. inhibition of receptor internalization and facilitation of beta 1-adrenergic receptor interaction with N-methyl-D-aspartate receptors. *J. Biol. Chem.*, **275**, 38659–38666.
Hurley, M.J., Mash, D.C. & Jenner, P. (2003) Expression of cannabinoid CB1 receptor mRNA in basal ganglia of normal and parkinsonian human brain. *J. Neural Transm.*, **110**, 1279–1288.
Ihalainen, J.A. & Tanila, H. (2004) In vivo regulation of dopamine and noradrenaline release by alpha2A-adrenoceptors in the mouse nucleus accumbens. *J. Neurochem.*, **91**, 49–56.
Jelsing, J., Galzin, A.M., Guillot, E., Pruniaux, M.P., Larsen, P.J. & Vrang, N. (2009) Localization and phenotypic characterization of brainstem neurons activated by rimonabant and WIN55,212-2. *Brain Res. Bull.*, **78**, 202–210.
Jentsch, J.D., Sanchez, D., Elsworth, J.D. & Roth, R.H. (2008) Clonidine and guanfacine attenuate phencyclidine-induced dopamine overflow in rat prefrontal cortex: mediating influence of the alpha-2A adrenoceptor subtype. *Brain Res.*, **1246**, 41–46.
Jongen-Relo, A.L., Voorn, P. & Groenewegen, H.J. (1994) Immunohistochemical characterization of the shell and core territories of the nucleus accumbens in the rat. *Eur. J. Neurosci.*, **6**, 1255–1264.
Kable, J.W., Murrin, L.C. & Bylund, D.B. (2000) In vivo gene modification elucidates subtype-specific functions of alpha(2)-adrenergic receptors. *J. Pharmacol. Exp. Ther.*, **293**, 1–7.
Kearn, C.S., Blake-Palmer, K., Daniel, E., Mackie, K. & Glass, M. (2005) Concurrent stimulation of cannabinoid CB1 and dopamine D2 receptors enhances heterodimer formation: a mechanism for receptor cross-talk? *Mol. Pharmacol.*, **67**, 1697–1704.
Kirigiti, P., Bai, Y., Yang, Y.F., Li, X., Li, B., Brewer, G. & Machida, C.A. (2001) Agonist-mediated down-regulation of rat beta1-adrenergic receptor transcripts: role of potential post-transcriptional degradation factors. *Mol. Pharmacol.*, **60**, 1308–1324.
Leweke, F.M. & Koethe, D. (2008) Cannabis and psychiatric disorders: it is not only addiction. *Addict. Biol.*, **13**, 264–275.
MacDonald, E., Kobilka, B.K. & Scheinin, M. (1997) Gene targeting – homing in on alpha 2-adrenoceptor-subtype function. *Trends Pharmacol. Sci.*, **18**, 211–219.
Mackie, K. (2005) Distribution of cannabinoid receptors in the central and peripheral nervous system. *Handb. Exp. Pharmacol.*, **168**, 299–325.
Maldonado, R., Valverde, O. & Berrendero, F. (2006) Involvement of the endocannabinoid system in drug addiction. *Trends Neurosci.*, **29**, 225–232.
Manzoni, O.J. & Bockaert, J. (2001) Cannabinoids inhibit GABAergic synaptic transmission in mice nucleus accumbens. *Eur. J. Pharmacol.*, **412**, R3–5.
Matyas, F., Yanovsky, Y., Mackie, K., Kelsch, W., Misgeld, U. & Freund, T.F. (2006) Subcellular localization of type 1 cannabinoid receptors in the rat basal ganglia. *Neuroscience*, **137**, 337–361.
Meana, J.J., Barturen, F. & Garcia-Sevilla, J.A. (1992) Alpha 2-adrenoceptors in the brain of suicide victims: increased receptor density associated with major depression. *Biol. Psychiatry*, **31**, 471–490.
Miner, L.H., Schroeter, S., Blakely, R.D. & Sesack, S.R. (2003) Ultrastructural localization of the norepinephrine transporter in superficial and deep layers of the rat prelimbic prefrontal cortex and its spatial relationship to probable dopamine terminals. *J. Comp. Neurol.*, **466**, 478–494.
Moranta, D., Esteban, S. & Garcia-Sevilla, J.A. (2009) Chronic treatment and withdrawal of the cannabinoid agonist WIN 55,212-2 modulate the sensitivity of presynaptic receptors involved in the regulation of monoamine syntheses in rat brain. *Naunyn Schmiedebergs Arch. Pharmacol.*, **379**, 61–72.
Moreira, F.A. & Lutz, B. (2008) The endocannabinoid system: emotion, learning and addiction. *Addict. Biol.*, **13**, 196–212.
Nissen, S.E., Nicholls, S.J., Wolski, K., Rodes-Cabau, J., Cannon, C.P., Deanfield, J.E., Despres, J.P., Kastelein, J.J., Steinhubl, S.R., Kapadia, S., Yasin, M., Ruzyllo, W., Gaudin, C., Job, B., Hu, B., Bhatt, D.L., Lincoff, A.M., Tuzcu, E.M. & STRADIVARIUS Investigators (2008) Effect of rimonabant on progression of atherosclerosis in patients with abdominal obesity and coronary artery disease: the STRADIVARIUS randomized controlled trial. *JAMA*, **299**, 1547–1560.
Nutt, D.J. (2002) The neuropharmacology of serotonin and noradrenaline in depression. *Int. Clin. Psychopharmacol.*, **17**(Suppl 1), S1–12.
Olson, V.G., Heusner, C.L., Bland, R.J., During, M.J., Weinshenker, D. & Palmiter, R.D. (2006) Role of noradrenergic signaling by the nucleus tractus solitarius in mediating opiate reward. *Science*, **311**, 1017–1020.
Oropeza, V.C., Page, M.E. & Van Bockstaele, E.J. (2005) Systemic administration of WIN 55,212-2 increases norepinephrine release in the rat frontal cortex. *Brain Res.*, **1046**, 45–54.
Oropeza, V.C., Mackie, K. & Van Bockstaele, E.J. (2007) Cannabinoid receptors are localized to noradrenergic axon terminals in the rat frontal cortex. *Brain Res.*, **1127**, 36–44.
Page, M.E., Oropeza, V.C., Sparks, S.E., Qian, Y., Menko, A.S. & Van Bockstaele, E.J. (2007) Repeated cannabinoid administration increases indices of noradrenergic activity in rats. *Pharmacol. Biochem. Behav.*, **86**, 162–168.
Paxinos, G. & Watson, C. (1997) *The Rat Brain in Stereotaxic Coordinates*. Academic Press, New York.
Peters, A.P., Palay, S.L. & Webster, H.D. (1991) *The Fine Structure of the Nervous System*. Oxford University Press, New York.
Pickel, V.M., Chan, J., Kash, T.L., Rodriguez, J.J. & MacKie, K. (2004) Compartment-specific localization of cannabinoid 1 (CB1) and mu-opioid receptors in rat nucleus accumbens. *Neuroscience*, **127**, 101–112.
Piomelli, D. (2003) The molecular logic of endocannabinoid signalling. *Nat. Rev. Neurosci.*, **4**, 873–884.

Ramos, B.P. & Arnsten, A.F. (2007) Adrenergic pharmacology and cognition: focus on the prefrontal cortex. *Pharmacol. Ther.*, **113**, 523–536.
Reyes, B. A. S., Rosario, J.C., Piana, P.M.T. & Van Bockstaele, E.J. (2009) Cannabinoid Modulation of cortical adrenergic receptors and transporters. *J. Neurosci. Res.*, **87**, 3671–3678.
Reynolds, S.M. & Berridge, K.C. (2001) Fear and feeding in the nucleus accumbens shell: rostrocaudal segregation of GABA-elicited defensive behavior versus eating behavior. *J. Neurosci.*, **21**, 3261–3270.
Reynolds, S.M. & Berridge, K.C. (2002) Positive and negative motivation in nucleus accumbens shell: bivalent rostrocaudal gradients for GABA-elicited eating, taste ''liking''/''disliking'' reactions, place preference/avoidance, and fear. *J. Neurosci.*, **22**, 7308–7320.
Reynolds, S.M. & Berridge, K.C. (2003) Glutamate motivational ensembles in nucleus accumbens: rostrocaudal shell gradients of fear and feeding. *Eur. J. Neurosci.*, **17**, 2187–2200.
Robbe, D., Alonso, G., Duchamp, F., Bockaert, J. & Manzoni, O.J. (2001) Localization and mechanisms of action of cannabinoid receptors at the glutamatergic synapses of the mouse nucleus accumbens. *J. Neurosci.*, **21**, 109–116.
Rodriguez de Fonseca, F., Del Arco, I., Martin-Calderon, J.L., Gorriti, M.A. & Navarro, M. (1998) Role of the endogenous cannabinoid system in the regulation of motor activity. *Neurobiol. Dis.*, **5**, 483–501.
Rudoy, C.A. & Van Bockstaele, E.J. (2007) Betaxolol, a selective beta(1)-adrenergic receptor antagonist, diminishes anxiety-like behavior during early withdrawal from chronic cocaine administration in rats. *Prog. Neuropsychopharmacol. Biol. Psychiatry*, **31**, 1119–1129.
Sanofi-Aventis Accomplia update. http://en.sanofiaventis.com/investors/events/corporate/2008/081023_investor_update.asp (accessed online 15 February 2009).
Shirayama, Y. & Chaki, S. (2006) Neurochemistry of the nucleus accumbens and its relevance to depression and antidepressant action in rodents. *Curr. Neuropharmacol.*, **4**, 277–291.
Strader, C.D., Pickel, V.M., Joh, T.H., Strohsacker, M.W., Shorr, R.G., Lefkowitz, R.J. & Caron, M.G. (1983) Antibodies to the beta-adrenergic receptor: attenuation of catecholamine-sensitive adenylate cyclase and demonstration of postsynaptic receptor localization in brain. *Proc. Natl. Acad. Sci. U S A*, **80**, 1840–1844.
Tan, Y., Williams, E.S. & Zahm, D.S. (1999) Calbindin-D 28kD immunofluorescence in ventral mesencephalic neurons labeled following injections of fluoro-gold in nucleus accumbens subterritories: inverse relationship relative to known neurotoxin vulnerabilities. *Brain Res.*, **844**, 67–77.
Teng, J., Takei, Y., Harada, A., Nakata, T., Chen, J. & Hirokawa, N. (2001) Synergistic effects of MAP2 and MAP1B knockout in neuronal migration, dendritic outgrowth, and microtubule organization. *J. Cell Biol.*, **155**, 65–76.
Tsou, K., Brown, S., Sanudo-Pena, M.C., Mackie, K. & Walker, J.M. (1998) Immunohistochemical distribution of cannabinoid CB1 receptors in the rat central nervous system. *Neuroscience*, **83**, 393–411.
Vasquez, C. & Lewis, D.L. (1999) The CB1 cannabinoid receptor can sequester G-proteins, making them unavailable to couple to other receptors. *J. Neurosci.*, **19**, 9271–9280.
Villares, J. (2007) Chronic use of marijuana decreases cannabinoid receptor binding and mRNA expression in the human brain. *Neuroscience*, **145**, 323–334.
Voorn, P., Gerfen, C.R. & Groenewegen, H.J. (1989) Compartmental organization of the ventral striatum of the rat: immunohistochemical distribution of enkephalin, substance P, dopamine, and calcium-binding protein. *J. Comp. Neurol.*, **289**, 189–201.
Wang, M., Ramos, B.P., Paspalas, C.D., Shu, Y., Simen, A., Duque, A., Vijayraghavan, S., Brennan, A., Dudley, A., Nou, E., Mazer, J.A., McCormick, D.A. & Arnsten, A.F. (2007) Alpha2A-adrenoceptors strengthen working memory networks by inhibiting cAMP-HCN channel signaling in prefrontal cortex. *Cell*, **129**, 397–410.
Witkin, J.M., Tzavara, E.T. & Nomikos, G.G. (2005) A role for cannabinoid CB1 receptors in mood and anxiety disorders. *Behav. Pharmacol.*, **16**, 315–331.
Zahm, D.S. (1999) Functional-anatomical implications of the nucleus accumbens core and shell subterritories. *Ann. N Y Acad. Sci.*, **877**, 113–128.